THE USE OF WAVELET TYPE BASIS FUNCTIONS IN THE MOM ANALYSIS OF MICROSTRIP STRUCTURES

A THESIS SUBMITTED TO
THE GRADUATE SCHOOL OF NATURAL AND APPLIED SCIENCES
OF
MIDDLE EAST TECHNICAL UNIVERSITY

BY

EMRE ÇAKIR

IN PARTIAL FULFILMENT OF THE REQUIREMENTS FOR
THE DEGREE OF MASTER OF SCIENCE
IN
ELECTRICAL AND ELECTRONICS ENGINEERING

DECEMBER 2004

Approval of the Graduate School of Natural and Applied Sciences

Prof. Dr. Canan ÖZGEN
Director

I certify that this thesis satisfies all the requirements as a thesis for the degree of Master of Science.

Prof. Dr. İsmet ERKMEN
Head of Department

This is to certify that we have read this thesis and that in our opinion it is fully adequate, in scope and quality, as a thesis for the degree of Master of Science.

Prof. Dr. Lale ALATAN
Supervisor

Examining Committee Members

Prof. Dr. Mustafa KUZUOGLU (METU, EE) _____

Assoc. Prof. Dr. Lale ALATAN (METU, EE) _____

Prof Dr. Adnan KÖKSAL (HACETTEPE, EE) _____

Assoc. Prof. Dr. Sencer KOÇ (METU, EE) _____

Assoc. Prof. Dr. Gülbin DURAL (METU, EE) _____

I hereby declare that all information in this document has been obtained and presented in accordance with academic rules and ethical conduct. I also declare that, as required by these rules and conduct, I have fully cited and referenced all material and results that are not original to this work.

Name, Last name : Emre ÇAKIR

Signature :

ABSTRACT

THE USE OF WAVELET TYPE BASIS FUNCTIONS IN THE MOM ANALYSIS OF MICROSTRIP STRUCTURES

ÇAKIR, Emre
M.S., Department of Electrical and Electronics Engineering
Supervisor: Assist. Prof. Dr. Lale ALATAN

December 2004, 78 pages

The Method of Moments (MoM) has been used extensively to solve electromagnetic problems. Its popularity is largely attributed to its adaptability to structures with various shapes and success in predicting the equivalent induced currents accurately. However, due to its dense matrix, especially for large structures, the MoM suffers from long matrix solution time and large storage requirement. In this thesis it is shown that use of wavelet basis functions result in a MoM matrix which is sparser than the one obtained by using traditional basis functions. A new wavelet system, different from the ones found in literature, is proposed. Stabilized Bi-Conjugate Gradient Method which is an iterative matrix solution method is utilized to solve the resulting sparse matrix equation. Both a one-dimensional problem with a microstrip line example and a two-dimensional problem with a rectangular patch antenna example are studied and the results are compared.

Key words: Method of Moments, sparse matrix, Wavelet basis functions, printed structures, microstrip antennas, Stabilized Bi-Conjugate Gradient Method.

ÖZ

MİKROŞERİT YAPILARDA DALGACIK TİPTEKİ TEMEL FONKSİYONLAR KULLANILARAK MOMENT METOD ANALİZİ

ÇAKIR, Emre
Yüksek Lisans, Elektrik ve Elektronik Mühendisliği Bölümü
Tez Yöneticisi: Y. Doç. Dr. Lale ALATAN

Aralık 2004, 78 Sayfa

Momentler Yöntemi (MoM), elektromanyetik problemlerin çözümünde kapsamlı olarak kullanılmaktadır. Bu yöntemin popülerliği büyük ölçüde, yapıların şekil değişikliklerinde uyum sağlamasına ve eşdeğer indüklene akımları hesaplamadaki başarısına dayanmaktadır. Bununla birlikte, yoğun sistem matrisinden dolayı, özellikle büyük yapılarda çözüm zamanının uzaması ve geniş hafızaya ihtiyaç duyulması MoM'u yetersiz kılmaktadır. Bu tezde MoM matrisinin oluşturulmasında alışılagelmiş temel fonksiyonlardan daha seyrek bir yapı meydana getiren dalgacık temel fonksiyonlarının kullanımı gösterilmiştir. Literatürde bulunanlardan farklı yeni bir dalgacık sistemi önerildi. Sonuçta bulunan seyrek matris denkleminin çözümünde bir döngülü çözüm yöntemi olan Stabilized Bi-Conjugate Gradient Metodu kullanıldı. Hem tek boyutlu mikroşerit hat örneği, hem de iki boyutlu dikdörtgen biçimindeki mikroşerit yama anten yapısı üzerinde çalışılarak, sonuçlar karşılaştırıldı.

Anahtar Kelimeler: Momentler Yöntemi, Seyrek Matris, Dalgacık temel fonksiyonları, Mikroşerit yapı, Stabilized Bi-Conjugate Gradient Metodu.

To My Family

ACKNOWLEDGMENTS

I wish to express my sincere gratitude to my advisor Assist. Prof. Dr. Lale ALATAN without whose support, this thesis would not have been possible. She carefully guided me throughout the pursuit of my Master's degree. Her ideas and suggestions have been invaluable to this thesis. I would like to thank her for being my advisor at METU.

I would like to express my sincere appreciation to Emre AĞIRNAS, Güney ÖZKAYA, Özkan ÜNVER and Timuçin BÜK for their valuable friendship, help and support.

I am also grateful to ASELSAN Inc. for facilities provided for the completion of this thesis.

Last in the list but first in my heart, I am grateful to my family, because they always supported emotionally and encouraged me when needed.

TABLE OF CONTENTS

LIST OF FIGURES

LIST OF TABLES

CHAPTER 1

INTRODUCTION

The number of applications involving electromagnetic scattering, coupling and wave propagation increases rapidly. In those applications, making a correct electromagnetic analysis and synthesis of the system is indispensable. Problems of this kind are generally formulated by linear integral or differential equations and solved by numerical techniques like method of Moments (MoM) [1], Finite Element Method (FEM) [2] and Finite Difference Time Domain Method (FDTD) [3].

With the growing popularity of printed structures, there has been a great deal of interest in developing accurate and efficient numerical techniques to analyze these structures. In the analysis of printed antennas, MoM is the most frequently used numerical method. In this method, the main purpose is to generate a matrix equation from a linear integral equation. To achieve this, first, the unknown function is approximated in terms of known basis functions and then by applying the boundary conditions with the help of testing functions, the weighted error due to this approximation is minimized [1]. The resultant matrix is generally a "dense" matrix. Because of the large memory requirement to store this dense matrix, MoM becomes inefficient for large scale scattering and radiation problems. In addition to the large memory requirement, the matrix solution time is another problem about large dense matrices. The number of operations used in the direct solution of a $N \times N$ dense matrix is $O(N^3)$. However, when a sparse matrix is considered, the solution can be obtained with less complexity by using iterative solution methods that works more efficiently for sparse matrices.

During the last decade many efforts have been done to reduce the complexity of the solution of the MoM matrix equation, but none of them achieved better than Multiresolution Analysis (MRA) [4] which will be studied in this thesis. As the name of the method implies, the analysis is performed at different resolution levels. While lower resolution levels offer a coarse resolution to the problem, the finer details are extracted at higher resolution levels. Such decomposition between different resolution levels can be achieved by using wavelet functions. Wavelet functions have some special features that will be discussed in detail. However the most important characteristic of wavelet functions is their zero average property. When wavelet type basis functions are used in the MoM analysis, the MoM matrix becomes sparse due to this characteristic. In this thesis, to improve the efficiency of the MoM solution of printed antennas, wavelet basis functions are used.

The wavelet functions are used in different areas of computational electromagnetics. Some of the examples of these studies that are related to this thesis can be found in [4] − [15].

Miller studies on the use of wavelet multiresolution analysis basis for producing the sparse matrix. The wavelet basis is implemented in the moment method matrix equation by direct expansion and application of the discrete wavelet transform. A comparison of different wavelets in the discrete wavelet transform implementation of a wavelet multiresolution analysis basis in the solution of the matrix equation is made. The Haar, Daubechies and Battle-Lemarie wavelets were chosen from among orthogonal wavelets. The linear spline and dual linear spline wavelets are semiorthogonal wavelets. Also the lower/upper decomposition direct solution method and the iterative biconjugate gradient are used to solve the matrix equations [4].

Sabet and Katehi developed an efficient space domain integral equation technique for the analysis of planar two- and three-dimensional dielectric structures. Orthonormal multiresolution expansions were employed in the moment method

solution of the integral equations. It was demonstrated that the use of a wavelet-dominated expansion basis leads to a highly sparse moment matrix. Also it is shown that the procedure of thresholding the moment matrix and the efficient iterative solvers can be used to speed up the computations dramatically. Then the formulation was applied to two typical 2D and 3D planar dielectric structures and the computational advantages of using multiresolution expansions over conventional basis functions have been discussed [5].

In [6], Steinberg and Leviatan studied the use of wavelet expansions in the MoM. They presented the theory of wavelet transforms in the MoM solution of electromagnetic wave interaction problems. They showed that the method is better suited for the analysis of scatterers which contain a broad spectrum of length scales ranging from a subwavelength to several wavelengths. Because wavelet expansion can adaptively fit itself to the various length scales associated with the scatterer by distributing the localized functions near the discontinuities and the more spatially diffused ones over the smooth parts of the scatterer. The performance of the proposed approach is illustrated by a numerical study of electromagnetic coupling through a double-slot aperture in a planar conducting screen separating two identical half-space regions.

Baharav and Leviatan worked on the impedance matrix compression (IMC) method for a more effective integration of wavelet-based transforms into existing numerical solvers. The feasibility of ensuring a slow growth in the number of unknowns even when there is a rapid increase in the problem complexity is shown by an illustrative example [7].

Wagner and Chew studied on the use of wavelet basis functions for the efficient solution of electromagnetic integral equations and analyzed radiation/receiving characteristics of the wavelet basis functions. Their results show that the use of classical wavelets (such as the Daubechies wavelets) does not appear to reduce the computational complexity of solving the problem but it will reduce the solution

time by a considerable factor. In addition, the sparsity produced by using wavelet basis functions is because of the nature of the fields radiated by the finest resolution wavelets. The wavelets with broader support have strong interactions with one another [8].

Wagner, Otto and Chew used wavelet like basis functions to produce a sparse MoM impedance matrix to solve the modes of an arbitrarily shaped hollow metallic waveguide using a surface integral equation/Method of Moments formulation. The obtained sparsity is used for fast solution of the problem and the same method is applied directly to the external scattering problem. They demonstrated that the use of wavelet-like basis functions reduced the MoM impedance matrix, Z, for a hollow metallic waveguide from N^2 nonzero elements in the pulse basis to αN^2 nonzero elements in the wavelet like basis, where $\alpha \approx 0.2$ for the examples considered [9].

In the solution of first-kind integral equations, Goswami, Chan and Chui used wavelets on a bounded interval. They used compactly supported semi-orthogonal spline wavelets specially constructed for the bounded interval in solving first kind integral equations. This technique is applied to analyze a problem involving two-dimensional electromagnetic scattering from metallic cylinders. According to the obtained results, some of the advantages of semi-orthogonal wavelets over orthonormal wavelets in numerical analysis have been discussed. The method was applied to evaluate the surface current distribution and radar cross section of an infinitely long metallic cylinder and the results of wavelet MoM have been found to be in good agreement with those of conventional MoM [10].

Tam, W.Y. used Haar wavelet, the most popular wavelet type, basis functions for transforming the dense impedance matrix to a sparse matrix using compactly supported wavelet-like basis functions. The simulations show the effects of the discretization size on the performance of the wavelet-like basis functions [11].

Sabet, Cheng and Katehi develop a wavelet-based formulation of the method of moments for the full-wave analysis of printed circuit antennas and arrays. Their approach is based on a system of planar space-domain integral equations for the unknown planar currents on the surface of radiating and feed elements. They used the wavelet type basis functions (B-spline wavelet in longitudinal direction, Haar wavelet in transverse direction) for the expansion of planar currents. It is shown that wavelet dominated expansion bases generate highly sparse moment matrices. The resulting sparse linear systems are solved numerically using very efficient computational tools [12].

An effective numerical method based on the wavelet matrix transforms for efficient solution of electromagnetic integral equations is proposed by Xiang and Lu. They used the wavelet matrix transform for producing highly sparse moment matrices which can be solved efficiently. The simulation results illustrated that nonorthonormal (Cardinal spline) wavelet transform that is obtained by using a fast construction method, results in higher compression rates and much more accurate results than using similarity wavelet transforms such as orthonormal (Daubechies) wavelet transform [13].

In this thesis a new set of wavelet basis functions are defined and they are used in the spatial domain MoM analysis of microstrip antennas. The results are compared to the ones obtained by using traditional rooftop basis functions.
This thesis is organized as follows. In the second chapter, Multiresolution Analysis is investigated. The method of defining the wavelet system with scaling and wavelet functions is explained. The concepts of orthogonality and semi-orthogonality for the wavelet sets are discussed.

In chapter 3, first the MoM solution of Mixed Potential Integral Equation (MPIE) used in the analysis of printed structures is summarized. Then, a review of the spatial domain closed form Green's functions for stratified media is given. The approach that is used for calculating the MoM matrix entries by using rooftop

basis functions is explained. Finally, two different methods namely the direct method and the Discrete Wavelet Transform (DWT) method used to calculate the MoM matrix by using wavelet basis functions are presented.

In chapter 4, the simulation results carried on MATLAB™ are presented. The degrees of sparsity obtained by using wavelet basis functions are demonstrated for different threshold levels and resolution levels. The results of the applied algorithm for the current distribution on the printed structure are illustrated for different resolution levels.

Finally, the conclusion part is provided in the last chapter.

CHAPTER 2

MULTIRESOLUTION ANALYSIS

In general, signals in their raw form are time-amplitude representations. These time domain signals are often needed to be transformed into other domains like frequency domain for analysis and processing. Depending on the application, the transformation technique is chosen, and each technique has its advantages and disadvantages.

In most applications, the frequency content of the signal is very important. The Fourier Transform (FT) is probably the most popular transform used to obtain the frequency spectrum of a signal. But the FT is only suitable for stationary signals whose frequency content does not change with time and it tells how much of each frequency exists in the signal, on the contrary it does not tell at which time these frequency components occur.

Most of the signals such as image signals, speech signals and also biological signals in nature are non-stationary. For analyzing these signals, both frequency and time information are needed, in other words, a time-frequency representation of the signal is necessary to solve this problem; the Short Time Fourier Transform was developed [16]. The main disadvantage of the STFT is that it uses a fixed window width. The STFT is a modified version of the Fourier Transform. The Fourier Transform separates the waveform into a sum of sinusoids of different frequencies and identifies their respective amplitudes. Thus it gives us a frequency-amplitude representation of the signal. In STFT, the non-stationary signal is divided into small portions, which are assumed to be stationary. This is done by using a window function of a chosen width, which is shifted and multiplied with the signal to obtain the small stationary signals. The Fourier

Transform is then applied to each of these portions to obtain the STFT of the signal. Once the window function is decided, the frequency and time resolutions are fixed for all frequencies and all times. So there is a trade-off between the time resolution and frequency resolution. If the chosen width of the window is narrow for assuming stationarity, frequency resolution becomes poor but we get good time resolution. If the width of the window is increased, the frequency resolution improves but time resolution becomes poor.

The Wavelet Transform solves the above problem by using short windows at high frequencies and long windows at low frequencies. This results in multiresolution analysis by which the signal is analyzed with different resolutions at different frequencies.

Wavelet analysis has attracted attention for its ability to analyze rapidly changing transient signals. Any application using the Fourier transform can be formulated using wavelets to provide more accurately localized temporal and frequency information. Wavelets are mathematical functions that cut up data into different frequency components, and then study each component with resolution matched to its scale [16], [17]. In Wavelet Transform, when frequency increases, the time resolution increases; the opposite situation is also true, when frequency decreases, the frequency resolution increases.

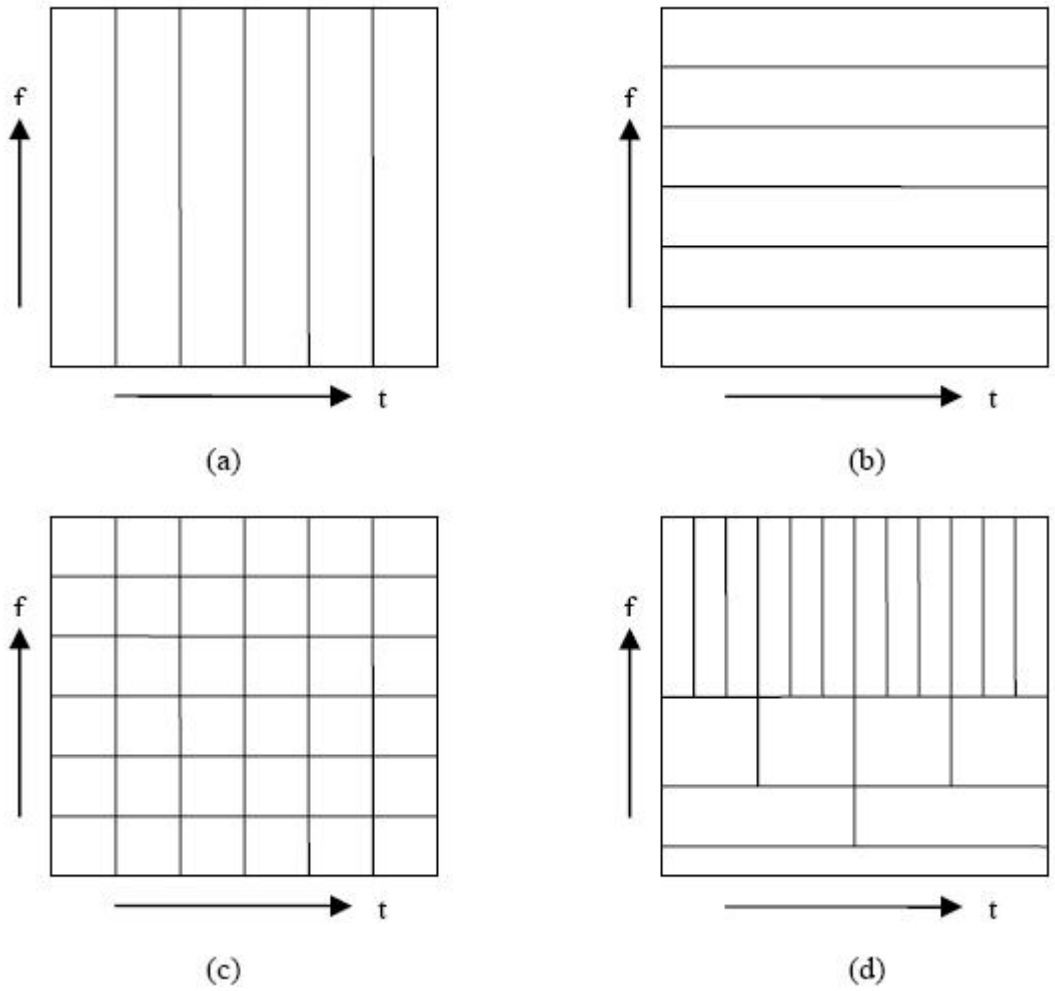

Figure 2-1 (a) Time Domain (b) Frequency domain (c) STFT (d) WT

Figure 2-1(a) shows only the time-domain plane of the time-frequency representation and does not give any frequency information, similarly Figure 2-1(b) shows only the frequency domain of the time-frequency representation and does not give any time information. Figure 2-1 (c) shows the STFT of the time-frequency representation and Figure 2-1 (d) shows the Wavelet Transform of the time-frequency representation. It is seen that STFT gives a fixed resolution at all times but Wavelet Transform gives a variable resolution.

In multiresolutional analysis, there are consecutive resolution levels in the form of a hierarchical tree. At each resolution level, the solution is decomposed into coarse and fine detail components. In the higher resolution level, the coarse part is again decomposed into two components. The coarse part of the solution is the slowly varying component therefore it corresponds to low frequency spectrum. On the other hand when fine details are investigated, rapid changes can be observed. Therefore details correspond to higher frequency components.

When a wavelet transform is used, a signal is separated into its low and high frequency components as shown in Figure 2.2 [18]. Low frequency approximation can be done by using scaling function, $\phi(x)$ and high frequency approximation can be done by using wavelet function, $\psi(x)$. These two functions must be designed carefully in order to achieve desired frequency extraction. In order to understand the idea of multi-resolution analysis, first of all, scaling function is analyzed and then the wavelet is defined in terms of it.

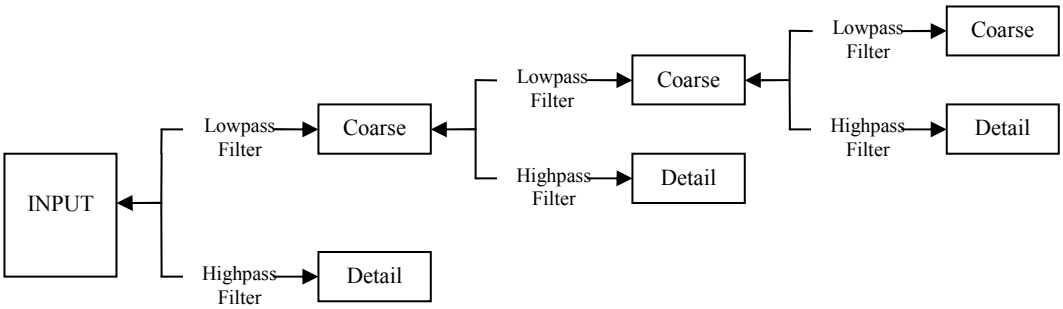

Figure 2-2 Wavelet Tree

2.1 Scaling Function

Scaling function is the main building block of a wavelet system. Both the set of scaling functions and wavelet functions at different resolution levels can be

obtained in terms of translations and dilations of the basic scaling function $\phi(x)$.Translation of the scaling function means shifting the function with an amount of k along the x axis as shown in Figure 2.3,

$$\phi_k(x) = \phi(x-k) \qquad k \in Z \qquad \phi \in L_2 \tag{2.1}$$

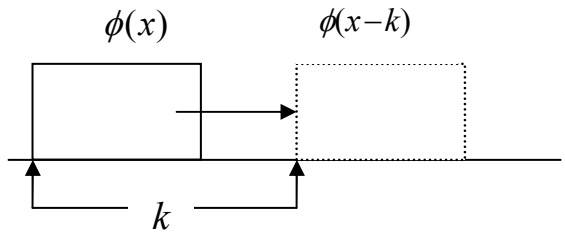

Figure 2-3 Translation of the Scaling Function

Dilation of the scaling function means changing the scale of the function by 2^j. Also it is shown in Figure 2.4 for j is equal to 0 and then 1 respectively.

$$\phi_j(x) = \phi(2^j x) \qquad j \in Z \qquad \phi \in L_2 \tag{2.2}$$

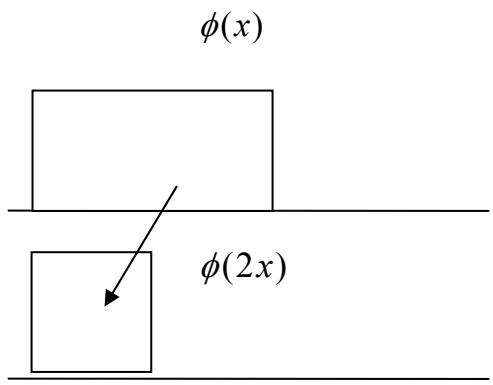

Figure 2-4 Dilation of the Scaling Function

Let V_j define the subspace of $L_2(R)$ which is spanned by these functions as follows

$$\phi_{j,k}(x) = 2^{j/2}\phi(2^j x - k) \qquad k = 0 \to 2^j - 1 \text{ and } j \geq 0 \tag{2.3}$$

$L_2(R)$ is the space of all functions $\phi(x)$ with a well defined integral of the square of the modulus of the function. The "L" signifies a Lebesque integral, the "2" denotes the integral of the square of the modulus of the function, and R states that the independent variable of integration x is a number over the whole real line.

The relationship between consecutive orders of subspaces can be shown as,

$$\cdots \subset V_{-2} \subset V_{-1} \subset V_0 \subset V_1 \subset V_2 \subset \cdots \subset L_2 \tag{2.4}$$

or

$$V_j \subset V_{j+1} \qquad \text{for all} \qquad j \in Z \tag{2.5}$$

with

$$V_{-\infty} = \{0\} \qquad\qquad V_{\infty} = L_2 \tag{2.6}$$

From the definition of V_j, the spaces have to satisfy

$$f(x) \in V_j \Leftrightarrow f(2x) \in V_{j+1} \tag{2.7}$$

which shows that elements in a space are scaled version of the elements in the next space.

From Figure 2.5, the space V_2 contains the two subspaces, W_1 and V_1. Also the subspace V_1 contains the two subspaces W_0 and V_0. The difference between the spaces that are spanned by the scaling functions forms the set spanned by the

wavelet functions (W_0, W_1). In the next section, the properties of wavelet functions will be discussed.

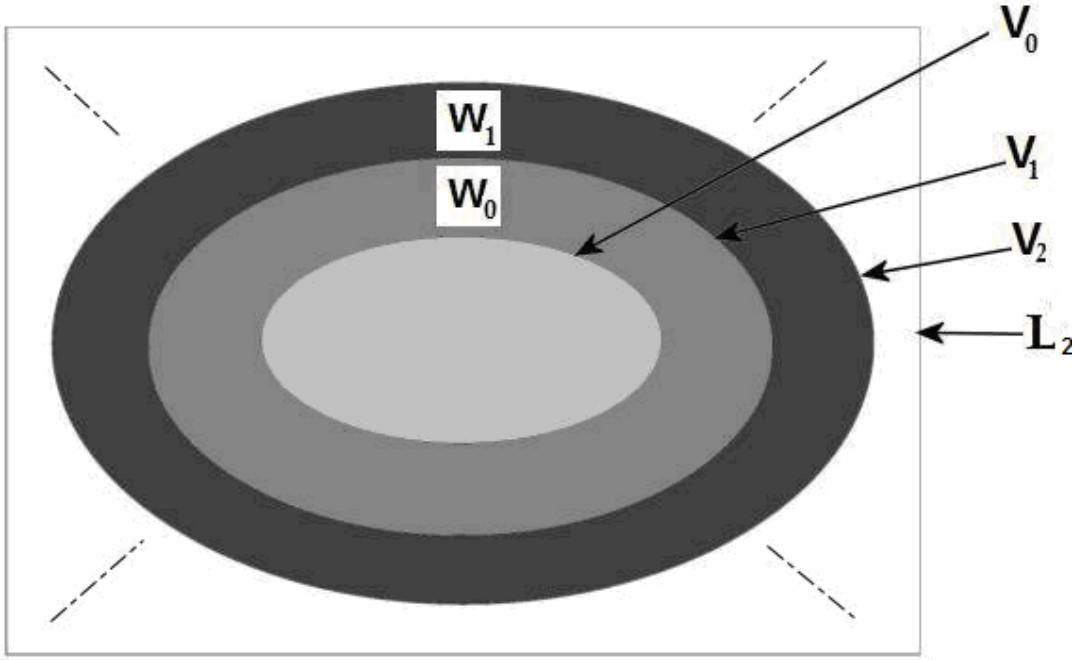

Figure 2-5 Nested vector spaces spanned by the scaling functions

2.2 Wavelet functions

Wavelet means a small wave. The small size refers to the length of the function. A wavelet is compactly supported, that means there is an interval outside which the wavelet is zero, or it has infinite support. However infinite support wavelets have exponential decay that allows them to be used like compactly supported wavelets [4]. The most important property of wavelets is that their average is zero which can be expressed mathematically as

$$\int_{-\infty}^{\infty} \psi(x)dx = 0 \tag{2.8}$$

After this brief introduction about wavelets, it will be better to return to the discussion about the relation between the wavelet functions and scaling function. A set of wavelet functions is constructed from the 'mother' wavelet by dilations and translations like scaling function. The term mother implies that the functions with different region of the support that are used in the transformation process are derived from one main function, or the mother wavelet. In other words, the mother wavelet is prototype for generating the other elements of the function set by dilations and translations as it is shown in Equation 2.9.

$$\psi_{j,k}(x) = 2^{j/2}\psi\left(2^{j/2} - k\right) \tag{2.9}$$

Let ψ_j define the subspace spanned by $\psi_{j,k}(x)$ for $k = 0 \rightarrow 2^j - 1$. Referring to Figure 2.5, it must be noticed that the two subspaces (V_0, W_1) are perpendicular to each other and any two wavelet subspaces are orthogonal to each other. As a result the wavelet sets at all resolution levels makes an orthonormal basis for $L_2(\Re)$.

From Figure 2.5 we can formulate the following extra expressions that show the relationship between the subspaces. $\oplus$ denotes the orthogonal sum.

$$V_1 = V_0 \oplus W_0 \tag{2.10}$$

$$V_2 = V_0 \oplus W_0 \oplus W_1 \tag{2.11}$$

$$L_2 = V_0 \oplus W_0 \oplus W_1 \oplus \cdots \tag{2.12}$$

The initial space is arbitrary, it can be chosen higher, and it means that the scaling function is at higher resolution level

$$L_2 = V_{10} \oplus W_{11} \oplus W_{12} \oplus W_{13} \cdots \tag{2.13}$$

or at a lower resolution level,

$$L_2 = V_{-5} \oplus W_{-5} \oplus W_{-4} \oplus W_{-3} \oplus \cdots \tag{2.14}$$

or for $j = -\infty$, the scaling function is eliminated as,

$$L_2 = \cdots W_{-2} \oplus W_{-1} \oplus W_0 \oplus W_1 \oplus W_2 \oplus \cdots \tag{2.15}$$

Figure 2.5 that summarizes the relation between the subspaces are very helpful in understanding the Multiresolution Analysis. Recall that behavior of a signal can be represented by using scaling functions and fine details are extracted by using wavelet functions. Therefore as we increase the resolution level, the rapidly varying wavelet functions will capture more details. By adding the details obtained at each resolution level $(\psi_j, \psi_{j+1}, \psi_{j+2}, \ldots)$ to the initial coarse behavior of the signal V_j, the overall signal can be obtained. Two illustrative examples presented in [17] are repeated here in Figures 2.6 and 2.7 to enhance the explanation about MRA. Figure 2.6 shows the scaling function approximations of Projection of The Houston Skyline Signal at various resolution levels. The component at the coarsest scale is simply the average of the signal. As the resolution level is increased by scaling the scale function, the approximation becomes close to the original signal. This is the traditional way of analyzing the signal. On the other hand, in Figure 2.7, MRA of Projection of The Houston Skyline Signal is illustrated. At each resolution level, more details are captured. As a result, the original signal that is illustrated in Figure 2.6 (h) can be summing up the projections onto the scaling and wavelet subspaces.

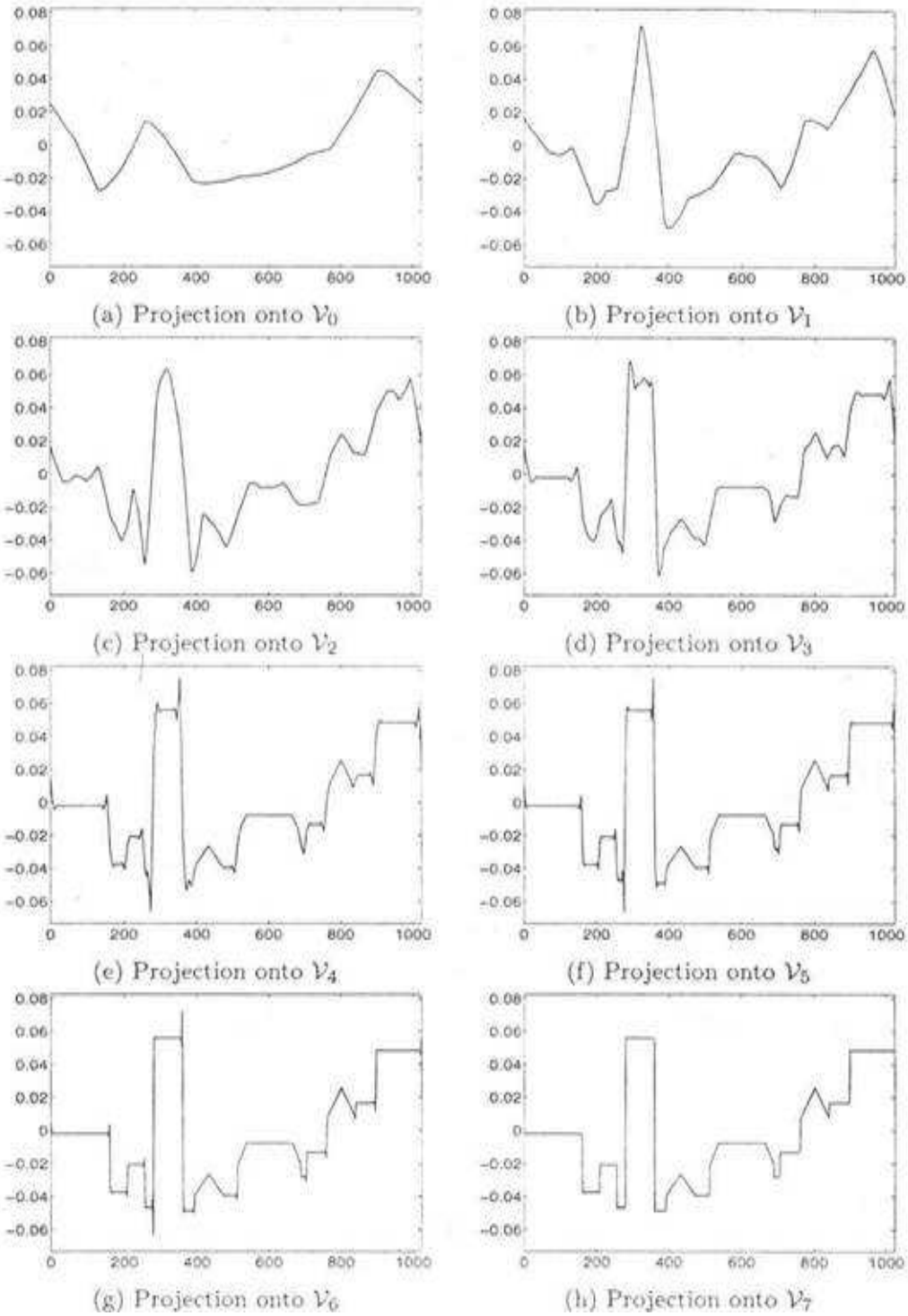

Figure 2-6 Projection of The Houston Skyline Signal onto ν spaces

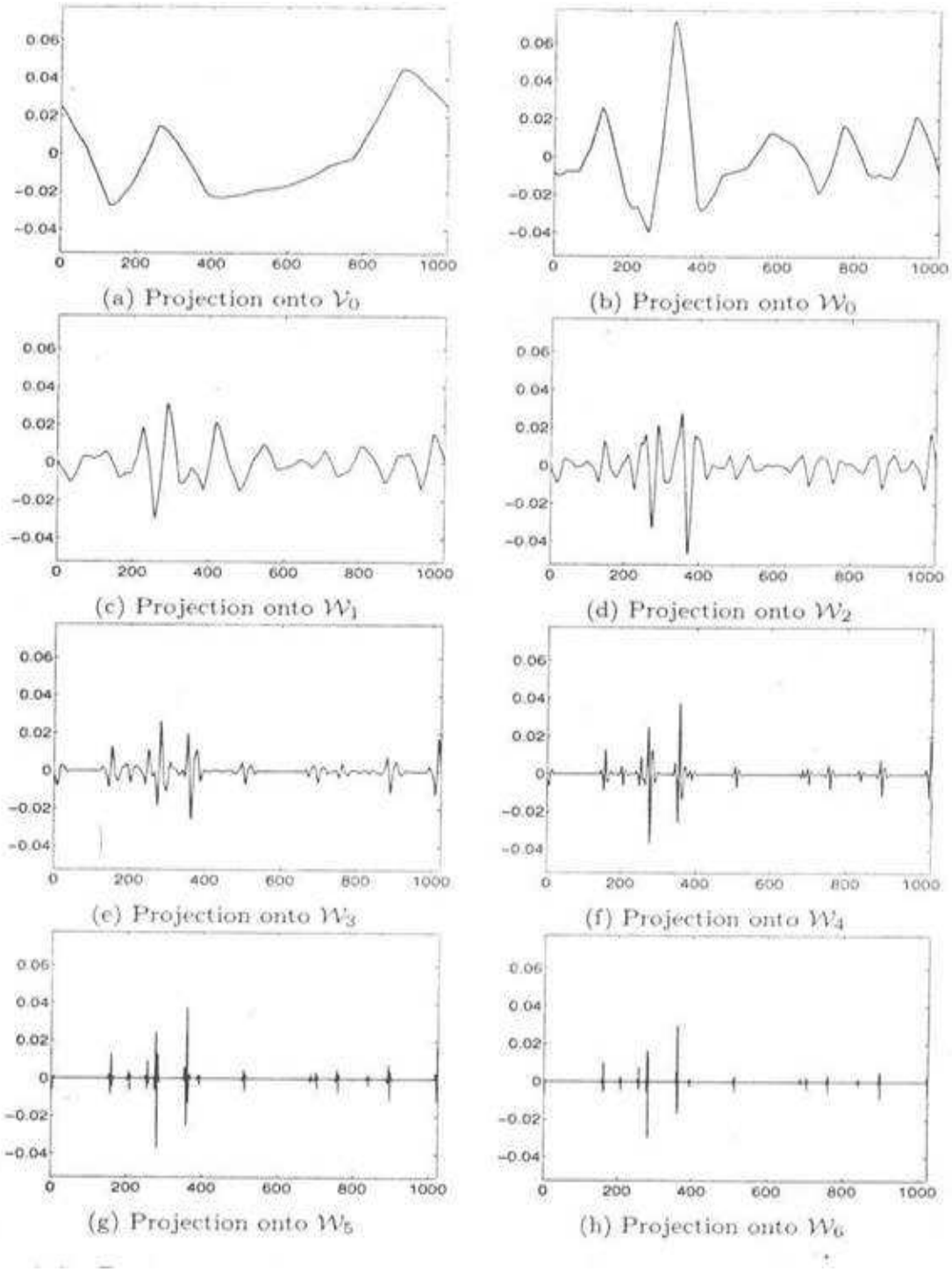

Figure 2-7 Projection of The Houston Skyline Signal onto W spaces

2.3 Orthogonal and Semi Orthogonal Wavelets

The most commonly used wavelet systems can be categorized into two classes: orthogonal and semi-orthogonal wavelets. An orthogonal family consists of sets of wavelets and scaling functions that are orthogonal to themselves and each other in dilation and translation on the same or different scales. A wavelet family is semi-orthogonal when its set of wavelets is orthogonal in dilations but not in translations. In this section, orthogonality and semi-orthogonality of the wavelets will be briefly discussed.

Orthogonal wavelets decompose signals into well-behaved orthogonal signal spaces. Orthogonality property is the most desired property in any signal analysis operation. For orthogonal wavelet systems with real functions, the following conditions should be satisfied [19].

Orthogonality: The wavelets $\{\psi_{j,k}\}$ form an orthogonal basis if

$$\psi_{j,k}(t).\psi_{m,n}(t)dt = \begin{cases} 1 & if \quad j = m \ and \ k = n \\ 0 & otherwise \end{cases} \tag{2.16}$$

$$\phi_{j,k}(t).\phi_{m,n}(t)dt = \begin{cases} 1 & if \quad j = m \ and \ k = n \\ 0 & otherwise \end{cases} \tag{2.17}$$

$$\phi_{j,k}(t).\psi_{m,n}(t)dt = 0 \quad for\ all\ j,k,m,n \tag{2.18}$$

Semi-Orthogonality: The wavelets $\{\psi_{j,k}\}$ form a semi-orthogonal basis if

$$\psi_{j,k}(t).\psi_{m,n}(t)dt = 0; \quad j \neq m \tag{2.19}$$

2.4 An Example of the Wavelet Systems: Haar Wavelets

In this section, mathematical discussion with a more complete example is given. In 1910, Haar showed that certain square wave functions could be translated and scaled to create a basis set that spans $L_2(R)$. This particular wavelet has been studied extensively in the image processing area as Haar transform. Graphs of Haar scaling function and mother wavelet are shown in Figure 2.8.

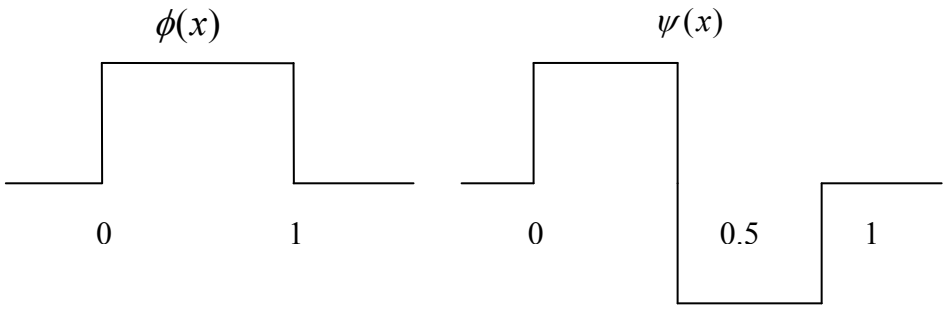

Figure 2-8 Scaling and mother Haar wavelet

A scaling function is a simple rectangle function

$$\phi(x) = \begin{cases} 1 & if \quad 0 < x < 1 \\ 0 & 0 \quad otherwise \end{cases} \tag{2.20}$$

and the wavelet be

$$\psi(x) = \begin{cases} 1 & for \quad 0 < x < 0.5 \\ -1 & for \quad 0.5 < x < 1 \\ 0 & \quad otherwise \end{cases} \tag{2.21}$$

The Haar functions are illustrated in Figure 2.9 where the first column contains the simple constant basis function that spans V_0, the second column contains the unit

pulse of width one half and the one translate necessary to span V_1. The third contains four translations of a pulse of width one fourth and the fourth contains eight translations of a pulse of width one eight. This shows clearly how increasing the scale allows better approximations to be realized.

V_0 is the space spanned by $\phi(x)$ which is a rather limited space. The next higher resolution space V_1 is spanned by $\phi(2x-k)$ which includes more class of signals than V_0. When higher values of j are given, the space V_j spanned by $\phi(2^j x-k)$ becomes better able to approximate arbitrary functions or signals.

However, using only the scaling function does not allow the high frequency (fine) – low frequency (coarse) decomposition, because of this reason, the wavelet is needed [4].

$\phi(2^j x-k)$

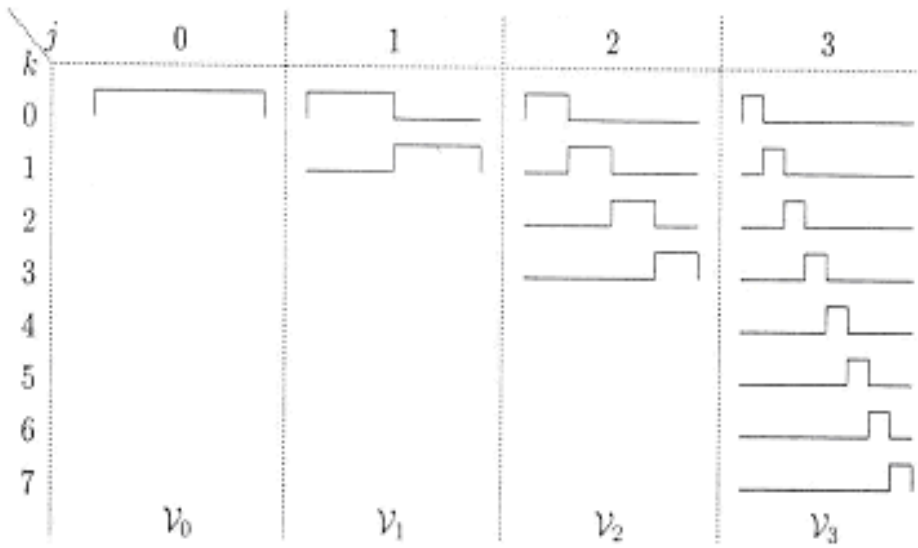

Figure 2-9 Haar Scaling Functions that Span Vj

Instead of using the scaling functions $\phi(8x-k)$ in V_3, the orthogonal decomposition is used

$$V_3 = V_2 \oplus W_2 \tag{2.22}$$

which is the same as

$$\overline{Span_k\{\phi(8x-k)\}} = \overline{Span_k\{\phi(4x-k)\}} \oplus \overline{Span_k\{\psi(4x-k)\}} \tag{2.23}$$

which means there are two sets of orthogonal basis functions that span V_3, one in terms of $j=3$ scaling functions, and the other in terms of half as many coarser $j=2$ scaling functions plus the details contained in the $j=2$ wavelets. This is illustrated in Figure 2.10.

The multiresolution character of the scaling function and wavelet system is easily seen from the Figure 2.10 where a signal in V_3 can be expressed in terms of a sum of eight shifted scaling functions at scale $j=3$ or a sum of four shifted scaling functions and four shifted wavelets at a scale of $j=2$.

The wavelet system introduced in this chapter will be used as the set of basis functions in the MoM analysis of printed structures. Hence, MoM formulation for planar microstrip circuits will be presented in the next chapter.

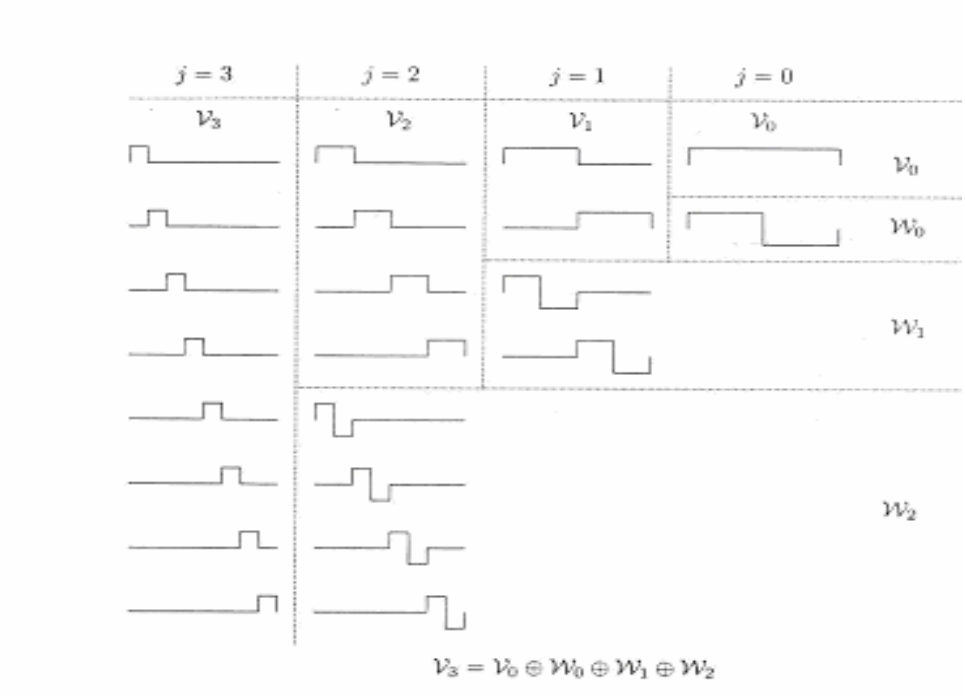

Figure 2-10 Haar scaling functions and wavelet decomposition of V_3

CHAPTER 3

THE ANALYSIS OF PLANAR PRINTED STRUCTURES

In this chapter, an introduction to the general microstrip structure is followed by its advantages and disadvantages. Next, the numerical method, MoM, is briefly discussed. Finally, a detailed application of the MoM to the analysis of microstrip structures is presented.

3.1 Microstrip Patch Antenna

In its most basic form, a microstrip patch antenna consists of a radiating patch on one side of a dielectric substrate which has a ground plane on the other side as shown in Figure 3.1.

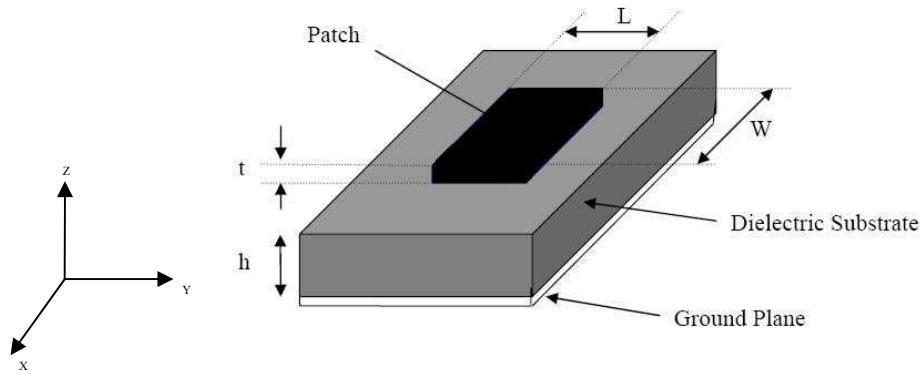

Figure 3-1 Structure of a Microstrip Patch Antenna

The patch is generally made of conducting material such as copper or gold and can take any possible shape, but it is generally square, rectangular, circular or triangular shape. Microstrip patch antennas radiate because of the fringing fields between the patch edge and the ground plane. In order to obtain a good antenna

performance, a thick dielectric substrate having a low dielectric constant is desirable since this provides better radiation and larger bandwidth [20]. However, such a configuration results in a larger antenna size. In order to design a compact microstrip patch antenna, higher dielectric constants must be used which are less efficient and narrower in bandwidth. Hence it is seen that there is a trade off between antenna dimensions and antenna performance.

3.2 Advantages and Disadvantages

Microstrip patch antennas are increasing in popularity for use in wireless applications due to their low-profile structure. Therefore they are extremely compatible for embedded antennas such as used in cellular phones. The communication antennas on missiles need to be thin and conformal and are often microstrip patch antennas. Another area where they have been used successfully is in satellite communication. Some of their principal advantages discussed by [20] and [21] are given below:

- Light weight and low volume
- Low fabrication cost, hence can be manufactured in large quantities.
- Supports both, linear as well as circular polarization.
- Can be easily integrated with microwave integrated circuits (MICs).
- Capable of dual and triple frequency operations.
- Mechanically robust when mounted on rigid surfaces.

Microstrip patch antennas suffer from a number of disadvantages as compared to conventional antennas. Some of the major disadvantages discussed by [20] and [21] are given below:

- Narrow bandwidth
- Low efficiency
- Low gain
- Surface wave excitation

Quality factor of an antenna, Q, represents the losses associated with the antenna. Microstrip patch antennas have a very high quality factor and for this reason they have narrow bandwidth and low efficiency.

3.3 Numerical solutions: Method of Moments

One of the methods, that provide the full wave analysis of microstrip patch antennas, is the Method of Moments. This is a numerical method used in various fields of engineering to solve integral or differential equations. The basic form of the equation to be solved by the Method of Moment is:

$$F(g(x)) = h(x) \tag{3.1}$$

where F is a known linear operator, g is an unknown function, and h is the source or excitation function. The aim here is to find g , when F and h are known. The unknown function g can be expanded as a linear combination of N terms to give:

$$g = \sum_{n=1}^{N} a_n g_n = a_1 g_1 + a_2 g_2 + \cdots + a_N g_N \tag{3.2}$$

where a_n is an unknown constant and g_n is a known function usually called a basis or expansion function. Substituting Equation (3.2) in (3.1) and using the linearity property of the operator F , (3.3) can be written, as

$$\sum_{n=1}^{N} a_n F(g_n(x)) = h(x) \tag{3.3}$$

A method of finding the constants, a_n, is the method of weighted residuals. In this method, a set of trial solutions is established with one or more variable parameters. The residuals are a measure of the difference between the trial solution and the true

solution. The variable parameters are selected in a way which guarantees a best fit of the trial functions based on the minimization of the residuals. This is done by defining a set of N weighting (or testing) functions $\{w_m\} = w_1, w_2, \ldots\ldots w_n$ in the domain of the operator F. Taking the inner product of these functions, Equation (3.3) becomes:

$$\sum_{n=1}^{N} a_n \langle w_m, F(g_n) \rangle = \langle w_m, h \rangle \tag{3.4}$$

where $m = 1,2,\ldots\ldots N$.

Writing in Matrix form,

$$[F_{mn}][a_n] = [h_m] \tag{3.5}$$

where

$$[F_m] = \begin{bmatrix} \langle w_1, F(g_1) \rangle & \langle w_1, F(g_2) \rangle & \cdots & \cdots \\ \langle w_2, F(g_1) \rangle & \langle w_2, F(g_2) \rangle & \cdots & \cdots \\ \vdots & & & \\ \vdots & & & \end{bmatrix} \tag{3.6}$$

$$[a_n] = \begin{bmatrix} a_1 \\ a_2 \\ a_3 \\ \vdots \\ a_N \end{bmatrix} \qquad [h_m] = \begin{bmatrix} \langle w_1, h \rangle \\ \langle w_2, h \rangle \\ \langle w_3, h \rangle \\ \vdots \\ \langle w_N, h \rangle \end{bmatrix} \tag{3.7}$$

It must be remembered that the weighting functions must be selected appropriately so that elements of $\{w_n\}$ are not only linearly independent but also minimize the computations required to evaluate the inner product. One such choice of the weighting functions may be to let the weighting and the basis function to be the

same, that is, $w_n = g_n$. This is called as the Galerkin's Method which is also used in this thesis.

3.4 Application of the MoM to the Analysis of Microstrip Structures

In order to analyze microstrip structures, an integral equation in terms of the induced currents that occur on the conducting surfaces should be obtained. For expressing the electric field, the scalar and vector potentials, ϕ and A, are used respectively.

$$\vec{E} = -j\omega\vec{A} - \nabla\phi \tag{3.8}$$

The vector and scalar potentials can be expressed in terms of the induced currents and Green's functions by using the convolution integrals where the convolution integral is denoted by *,

$$\vec{A} = \overline{\overline{G}}^{A} * \vec{J} \tag{3.9}$$

$$\phi = G_q * \left(-\frac{1}{j\omega} \nabla . \vec{J} \right) \tag{3.10}$$

$\overline{\overline{G}}^{A}$ is the dyadic Green's function of the vector potential, G_q is the Green's function of the scalar potential, $\vec{J} = J_x \hat{a}_x + J_y \hat{a}_y$ is the surface current density. The integral equation form of (3.9) can also be written as

$$\overline{\overline{G}}^{A} * \vec{J} = \iint_S \overline{\overline{G}}^{A} (x - x', y - y') \cdot \vec{J}(x', y') dx' dy' \tag{3.11}$$

Substituting (3.9) and (3.10) into (3.8) and using the condition that the tangential electric field on the perfect electric conductors (at patch surface) should be zero, the following integral equations are obtained,

$$-E_x^{inc} = -j\omega G_{xx}^A * J_x + \frac{1}{j\omega}\frac{1}{\partial x}\left[G_q * \nabla.\vec{J}\right] \tag{3.12}$$

$$-E_y^{inc} = -j\omega G_{yy}^A * J_x + \frac{1}{j\omega}\frac{1}{\partial y}\left[G_q * \nabla.\vec{J}\right] \tag{3.13}$$

where E_x^{inc} and E_y^{inc} are the x and y components of the incident electric field due to the source (or excitation) current, $\vec{J}_S$, respectively.

To solve the integral equations in (3.12) and (3.13) by using MoM, first, the induced current density is expanded in terms of the basis functions J_{xn} and J_{yn} as

$$J_x = \sum_{n=1}^{N} A_n J_{xn}(x, y) \tag{3.14}$$

$$J_y = \sum_{n=1}^{N} B_n J_{yn}(x, y) \tag{3.15}$$

Then, the boundary conditions are applied in integral sense with the use of the testing functions T_{xn} and T_{yn} through a proper choice of inner product

$$\langle f, g \rangle = \int_{-\infty}^{\infty}\int f^*(x, y) g(x, y) dxdy \tag{3.16}$$

Hence the following matrix equation is obtained

$$\begin{bmatrix} Z_{mn}^{xx} & Z_{mn}^{xy} \\ Z_{mn}^{yx} & Z_{mn}^{yy} \end{bmatrix} \begin{bmatrix} A_n \\ B_n \end{bmatrix} = \begin{bmatrix} V_m^x \\ V_m^y \end{bmatrix} \tag{3.17}$$

where

$$Z_{mn}^{xx} = \left\langle T_{xm}, G_{xx}^A * J_{xn} \right\rangle + \frac{1}{\omega^2} \left\langle T_{xm}, \frac{\partial}{\partial x} \left[G_q * \frac{\partial}{\partial x} J_{xn} \right] \right\rangle \tag{3.18}$$

$$Z_{mn}^{yy} = \left\langle T_{ym}, G_{yy}^A * J_{yn} \right\rangle + \frac{1}{\omega^2} \left\langle T_{ym}, \frac{\partial}{\partial y} \left[G_q * \frac{\partial}{\partial y} J_{yn} \right] \right\rangle \tag{3.19}$$

$$Z_{mn}^{xy} = \frac{1}{\omega^2} \left\langle T_{xm}, \frac{\partial}{\partial x} \left[G_q * \frac{\partial}{\partial y} J_{yn} \right] \right\rangle \tag{3.20}$$

$$Z_{mn}^{yx} = \frac{1}{\omega^2} \left\langle T_{ym}, \frac{\partial}{\partial y} \left[G_q * \frac{\partial}{\partial x} J_{xn} \right] \right\rangle \tag{3.21}$$

$$V_m^x = -\left\langle T_{xm}, E_x^{inc} \right\rangle \tag{3.22}$$

$$V_m^y = -\left\langle T_{ym}, E_y^{inc} \right\rangle \tag{3.23}$$

After a change of variables and the use of integration by parts the matrix entries can be expressed in the more convenient forms as follows;

$$Z_{mn}^{xx} = \iint dudv G_{xx}^A \left[T_{xm} \otimes J_{xn} \right] - \frac{1}{\omega^2} \iint dudv G_q \left[\frac{\partial}{\partial x} T_{xm} \otimes \frac{\partial}{\partial x} J_{xn} \right] \tag{3.24}$$

$$Z_{mn}^{xy} = -\frac{1}{\omega^2} \iint dudv G_q \left[\frac{\partial}{\partial x} T_{xm} \otimes \frac{\partial}{\partial y} J_{yn} \right] \tag{3.25}$$

$\otimes$ denotes the correlation function.

As the correlation of the basis and testing functions can be obtained analytically, the calculation of the matrix entries requires the numerical evaluation of two-dimensional (2-D) integrals over finite domains. However, these integrals involve the spatial-domain Green's functions which can be obtained from their spectral domain counterparts that can be derived analytically for planar multilayer media, via Hankel transformation, also called Sommerfeld integral. Since the kernel of the transformation is the Bessel function of the first kind and the function to be transformed is the spectral domain Green's function, the integrand is an oscillatory and slow-converging function. Therefore, the calculation of the spatial domain Green's function, i.e., the numerical implementation of the Hankel transformation, is the computational bottleneck of the spatial domain MoM. To remedy this difficulty, the closed-form Green's functions method is used [22]. In this method, first the spectral domain Green's functions are approximated by complex exponentials through the use of Generalized Pencil of Function (GPOF) method as follows;

$$\widetilde{G} \cong \frac{1}{j2k_Z}\left(\sum_{n=1}^{N_1} a_{1n} e^{-\alpha_{1n} k_z} + \sum_{n=1}^{N_2} a_{2n} e^{-\alpha_{2n} k_z}\right) \tag{3-26}$$

where a_{1n}, α_{1n} and a_{2n}, α_{2n} are the coefficients and exponents obtained from the application of the GPOF method in the first and second parts of the two-level approximation, respectively [23]. Then, the spatial domain Green's function is written in the following form by using the Weyl identity.

$$G \cong \sum_{n=1}^{N_1} a_{1n} \frac{e^{-jk_s r_{1n}}}{r_{1n}} + \sum_{n=1}^{N_2} a_{2n} \frac{e^{-jk_s r_{2n}}}{r_{2n}} \tag{3-27}$$

where $r_{1n} = \sqrt{x^2 + y^2 - \alpha_{1n}^2}$ and $r_{2n} = \sqrt{x^2 + y^2 - \alpha_{2n}^2}$ are the complex distances and k_s is the wave number in the source medium.

3.5 Rooftop Basis Functions

To guarantee the convergence of integrals appearing in the MoM matrix entries, the testing function should be at least piecewise continuous and the basis function should be at least piecewise differentiable in the longitudinal direction [24]. Since the Galerkin's procedure is used, the basis and the testing function must be the same. Therefore rooftop basis functions which are triangular in longitudinal direction and constant in the transverse direction are generally used as both the basis and the testing functions. The shape of the rooftop basis function is shown in Figure 3.2 and its mathematical expressions are given in Equations (3-28) and (3-29).

$$J_x^{nm}(x)=\begin{cases} \frac{1}{h_x}(x-x_n)+1 & x_{n-1}<x<x_n \\ -\frac{1}{h_x}(x-x_n)+1 & x_n<x<x_{n+1} \\ 0 & otherwise \end{cases} \tag{3.28}$$

$$J_x^{nm}(y)=\begin{cases} 1 & y_{m-1}<y<y_m \\ 0 & otherwise \end{cases} \tag{3.29}$$

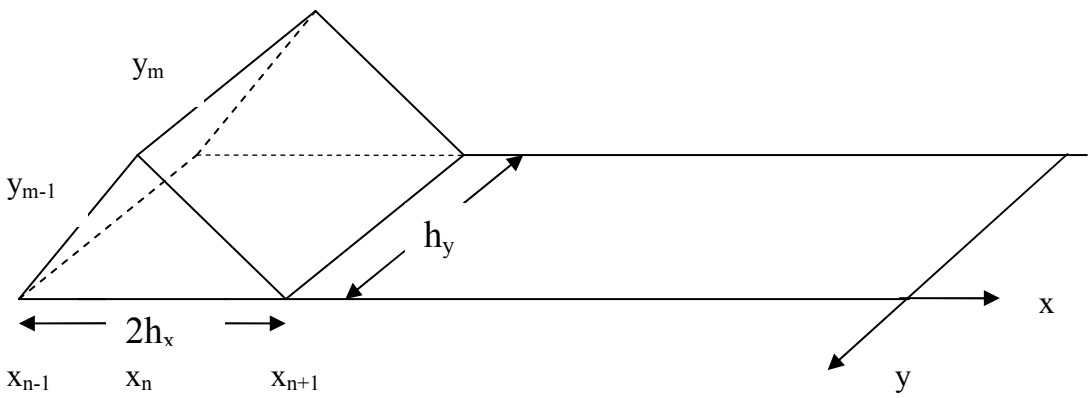

Figure 3-2 Rooftop Basis Functions

3.6 Choice of Wavelet System

While choosing an appropriate wavelet system to be used as basis functions for the expansion of surface currents, the following subjects should be considered.

- Current should be zero at the edges in the longitudinal direction. Therefore a compactly supported basis function with zero value at the end points is needed.

- For the convergence of the integrals involving derivatives of basis and testing functions, they should be at least piecewise differentiable.

- Matrix entries involve integrals of basis and testing functions. The numerical evaluation of these integrals would converge more easily if linear functions are chosen as opposed to higher order polynomial like functions. Therefore highly oscillatory functions like Daubechies wavelets are not preferred.

- If the chosen wavelet functions could be expressed in terms of rooftop basis functions, then instead of constructing the MoM matrix for the wavelet system by directly evaluating each entry, it can be obtained from the matrix already obtained by the rooftop basis functions through simple matrix evaluations.

In the light of the above discussion, the scaling function and the wavelet functions defined in Figure 3-3 and Figure 3-4 are chosen in the longitudinal direction and the Haar wavelet function is chosen in the transverse direction as given in Figure 2-8.

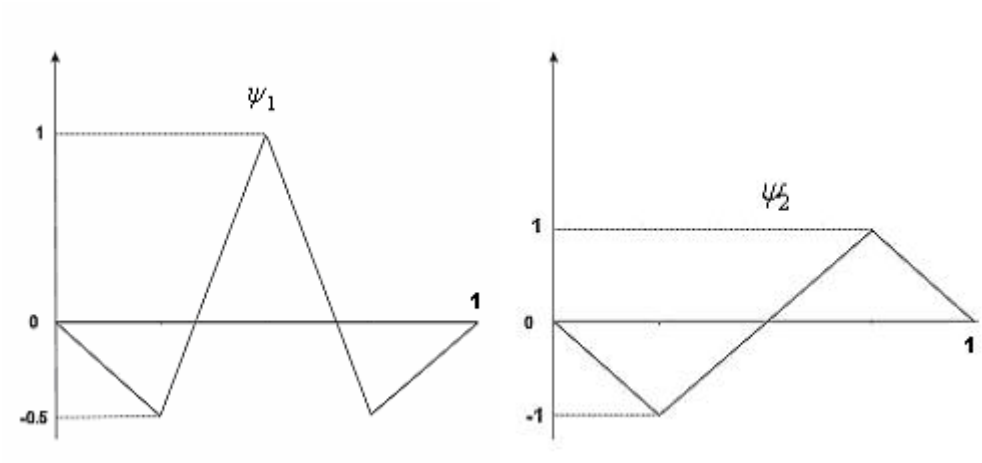

Figure 3-3 Defined Wavelets

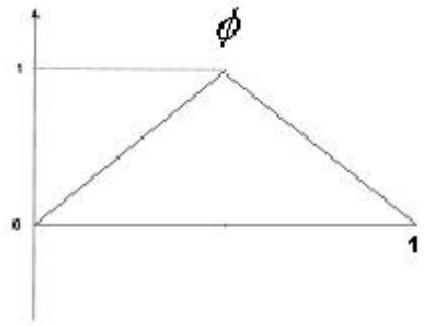

Figure 3-4 Defined Scaling Function

The reason for choosing two wavelet functions is to be able to span the same set as the roof-top functions. Consider the case that solution space is divided into two subdomains. In that case three rooftop basis functions should be used as shown in Figure 3.5.

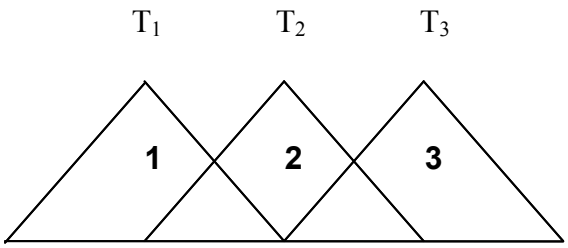

Figure 3-5 Three Rooftop Basis Functions

In Figures 3.6 – 3.9, the construction of each roof-top basis function by using the scaling and wavelet functions are illustrated.

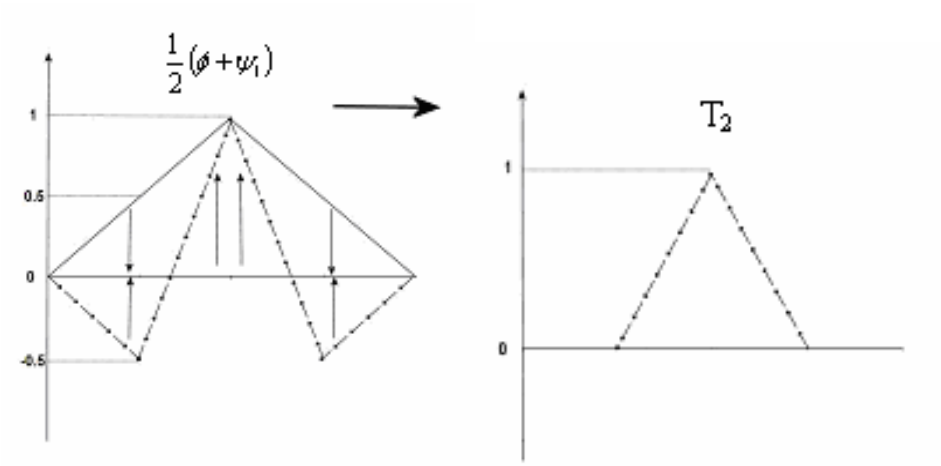

Figure 3-6 The Construction of Second Roof-top Basis Function

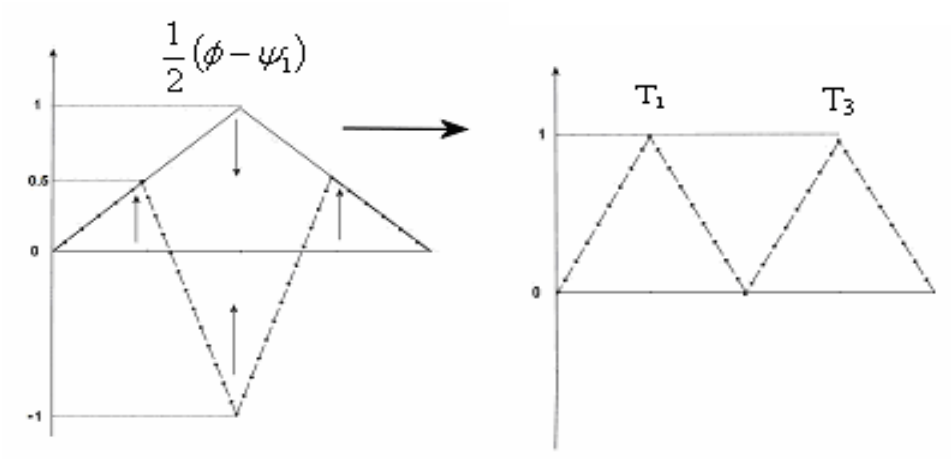

Figure 3-7 The Construction of First and Third Roof-top Basis Functions

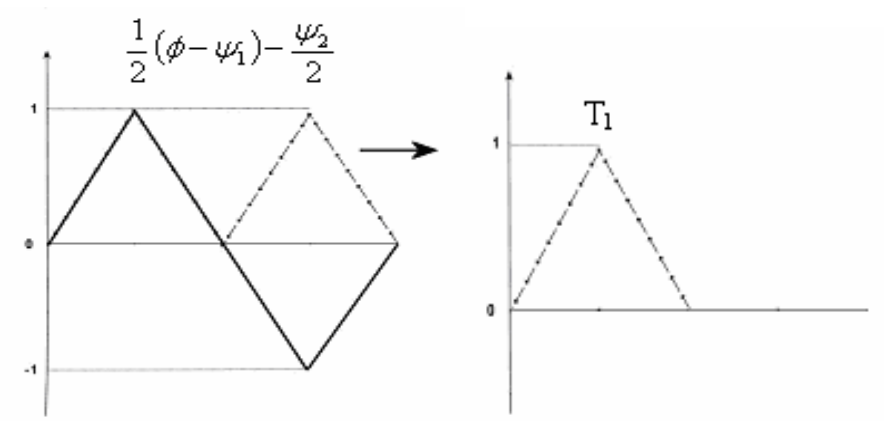

Figure 3-8 The Construction of First Roof-top Basis Functions

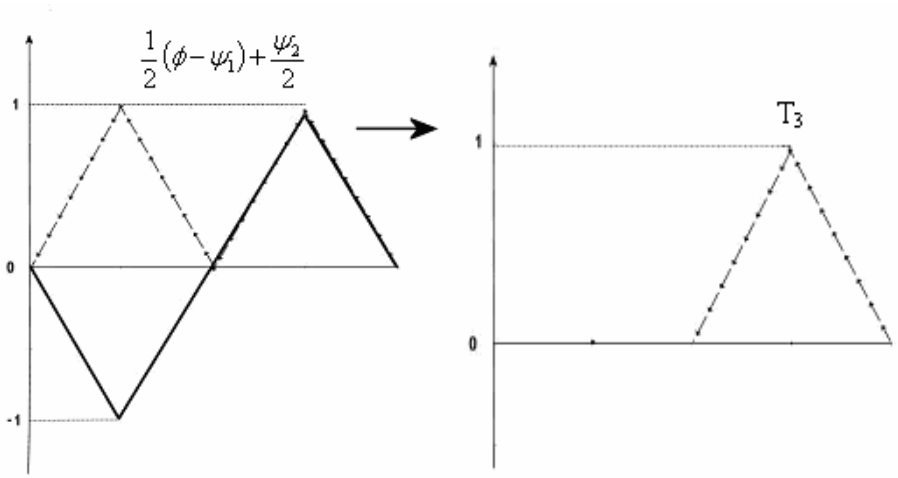

Figure 3-9 The Construction of Third Roof-top Basis Functions

As a result, it can be concluded that any signal that can be represented in terms of T_1, T_2 and T_3 can also be written as a linear combination of ϕ, ψ_1 and ψ_2. The level decomposition for the wavelet system adopted in this thesis is summarized in Figure 3-10

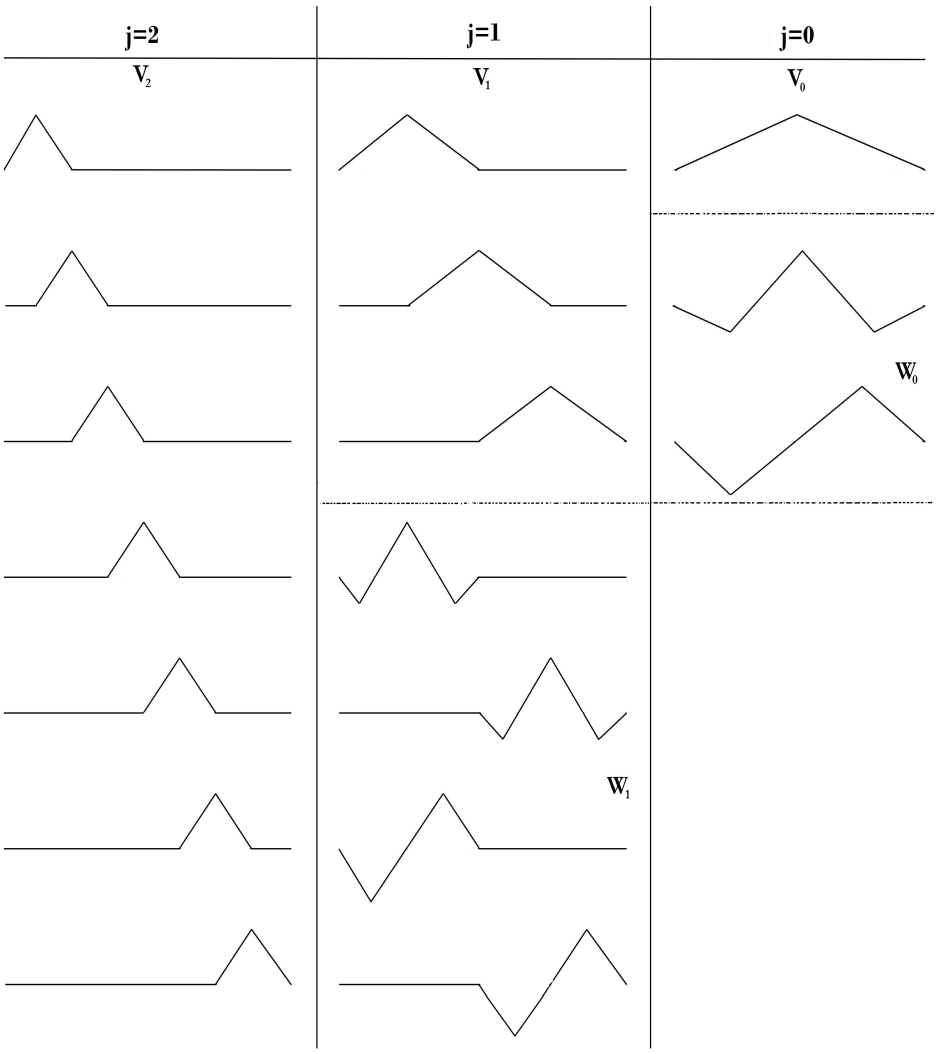

Figure 3-10 Wavelet Decomposition

$$V_2 = V_0 + W_0 + W_1 \quad \text{or} \quad V_1 = V_0 + W_0 \tag{3.30}$$

3.7 Construction of the MoM matrix with wavelet basis functions

Wavelets can be applied by the direct expansion method or by performing a Discrete Wavelet Transform (DWT) on the matrix equation generated by another basis and testing set, usually pulse expansion and delta testing or pulse expansion and pulse testing. The direct way to combine wavelets and MoM is to use the wavelet set as the basis and testing sets. The generated wavelet impedance matrix by direct method is given in (3.38). An alternative way to apply wavelet basis into the MoM solution of the integral equation is DWT.

Following is the matrix equation obtained by using rooftop basis and testing functions

$$Zi = v \tag{3.31}$$

Define a transformation matrix W where each row of W corresponds to the coefficients used to express each wavelet basis in terms of rooftop basis functions. Then the matrix equation for the wavelet basis and testing functions can be obtained as follows:

$$WZW^T(W^T)^{-1}i = Wv \tag{3.32}$$

$$\hat{Z} = WZW^T \tag{3.33}$$

$$\hat{i} = \left(W^T\right)^{-1} i \tag{3.34}$$

$$\hat{v} = Wv \tag{3.35}$$

$$\hat{Z}\hat{i} = \hat{v} \tag{3.36}$$

The above procedure is called DWT. For example for the triangular wavelet system defined in the previous section with ϕ, ψ_1 and ψ_2 the transform matrix becomes

$$W = \begin{bmatrix} \frac{1}{2} & 1 & \frac{1}{2} \\ -\frac{1}{2} & 1 & -\frac{1}{2} \\ -1 & 0 & 1 \end{bmatrix} \tag{3.37}$$

To demonstrate the equivalence of the direct evaluation of the matrix entries and the DWT methods, Haar wavelet system will be used as an example because of its simplicity.

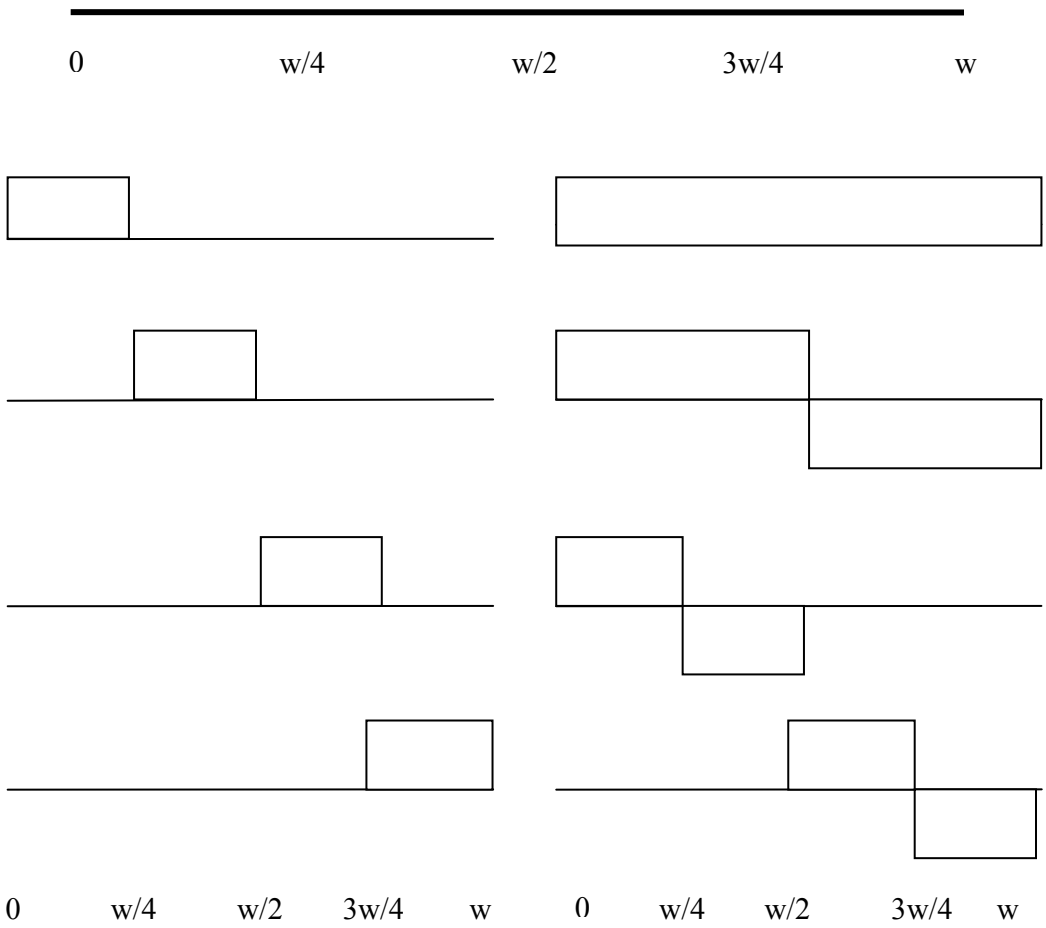

Figure 3-11 The left side shows the subdomain pulse basis. The right side shows the Haar wavelet MRA basis.

In Figure 3.11, the difference between the wavelet basis set and a classical subdomain basis set is shown. The subdomain basis is on the left and the wavelet MRA is shown on the right. The wavelet MRA is made of two functions, the wavelet and scaling function, and the wavelet function exists at the different resolution levels.

The wavelet impedance matrix for this example is composed of the following elements

$$\begin{bmatrix}
\int_0^w\int_0^w dK & \int_0^w\left[\int_0^{w/2} - \int_{w/2}^{w}\right]dK & \int_0^w\left[\int_0^{w/4} - \int_{w/4}^{w/2}\right]dK & \int_0^w\left[\int_{w/2}^{3w/4} - \int_{3w/4}^{w}\right]dK \\
\left[\int_0^{w/2} - \int_{w/2}^{w}\right]\int_0^w dK & \left[\int_0^{w/2} - \int_{w/2}^{w}\right]\left[\int_0^{w/2} - \int_{w/2}^{w}\right]dK & \left[\int_0^{w/2} - \int_{w/2}^{w}\right]\left[\int_0^{w/4} - \int_{w/4}^{w/2}\right]dK & \left[\int_0^{w/2} - \int_{w/2}^{w}\right]\left[\int_0^{3w/4} - \int_{3w/4}^{w}\right]dK \\
\left[\int_0^{w/4} - \int_{w/4}^{w/2}\right]\int_0^w dK & \left[\int_0^{w/4} - \int_{w/4}^{w/2}\right]\left[\int_0^{w/2} - \int_{w/2}^{w}\right]dK & \left[\int_0^{w/4} - \int_{w/4}^{w/2}\right]\left[\int_0^{w/4} - \int_{w/4}^{w/2}\right]dK & \left[\int_0^{w/4} - \int_{w/4}^{w/2}\right]\left[\int_{w/2}^{3w/4} - \int_{3w/4}^{w}\right]dK \\
\left[\int_{w/2}^{3w/4} - \int_{3w/4}^{w}\right]\int_0^w dK & \left[\int_0^{3w/4} - \int_{3w/4}^{w}\right]\left[\int_0^{w/2} - \int_{w/2}^{w}\right]dK & \left[\int_{w/2}^{3w/4} - \int_{3w/4}^{w}\right]\left[\int_0^{w/4} - \int_{w/4}^{w/2}\right]dK & \left[\int_{w/2}^{3w/4} - \int_{3w/4}^{w}\right]\left[\int_{w/2}^{3w/4} - \int_{3w/4}^{w}\right]dK
\end{bmatrix} \tag{3.38}$$

Also the pulse impedance matrix is given in the following equation for comparison.

$$\begin{bmatrix} \int_0^{w/4}\int_0^{w/4} dK & \int_0^{w/4}\int_{w/4}^{w/2} dK & \int_0^{w/4}\int_{w/2}^{3w/4} dK & \int_0^{w/4}\int_{3w/4}^{w} dK \\ \int_{w/4}^{w/2}\int_0^{w/4} dK & \int_{w/4}^{w/2}\int_{w/4}^{w/2} dK & \int_{w/4}^{w/2}\int_{w/2}^{3w/4} dK & \int_{w/4}^{w/2}\int_{3w/4}^{w} dK \\ \int_{w/2}^{3w/4}\int_0^{w/4} dK & \int_{w/2}^{3w/4}\int_{w/4}^{w/2} dK & \int_{w/2}^{3w/4}\int_{w/2}^{3w/4} dK & \int_{w/2}^{3w/4}\int_{3w/4}^{w} dK \\ \int_{3w/4}^{w}\int_0^{w/4} dK & \int_{3w/4}^{w}\int_{w/4}^{w/2} dK & \int_{3w/4}^{w}\int_{w/2}^{3w/4} dK & \int_{3w/4}^{w}\int_{3w/4}^{w} dK \end{bmatrix} \tag{3.39}$$

$$W = \begin{bmatrix} 1 & 1 & 1 & 1 \\ 1 & 1 & -1 & -1 \\ 1 & -1 & 0 & 0 \\ 0 & 0 & 1 & -1 \end{bmatrix} \tag{3.40}$$

When we substitute (3.39) and (3.40) in Equation (3.33), we can get the directly computed impedance matrix given in (3.38). This example demonstrates that in order to decrease the complexity of the computations, it is better to obtain the MoM matrix for the wavelet basis by using DWT method instead of directly computing it.

CHAPTER 4

SIMULATION RESULTS AND DISCUSSIONS

In this section, the results of computer simulations are presented to investigate the performance of wavelet type basis and testing functions used in the MoM analysis of microstrip lines and rectangular microstrip patch antennas. First the microstrip line example is studied since it is a simpler geometry due to its one dimensional structure.

In Figure 4.1 the basic concept of the construction of the transformed MoM matrix is illustrated. When the transformed MoM matrix is obtained, the important part of our problem is solved. To obtain a sparse matrix, first a threshold value relative to the maximum of the matrix elements is chosen. Then, the matrix entries that are smaller than this threshold value are replaced with zero value.

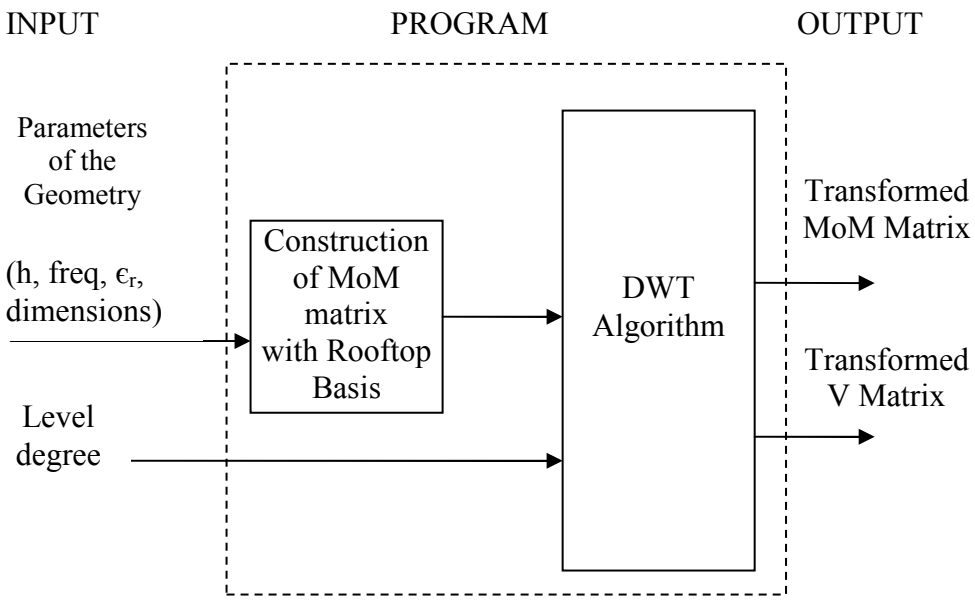

Figure 4-1 DWT Algorithm

A microstrip line is divided into 64 subdomains that results in 63 rooftop basis functions. For the wavelet system this division corresponds to resolution level j=5. In Figure 4.2 (a), the sparsity pattern of the wavelet transform matrix, W, that is used in DWT is illustrated. Each row of the transform matrix stands for coefficients of rooftop basis functions to construct the corresponding wavelet function. In order to demonstrate the indexing procedure of the wavelet system the first 7 wavelet functions are shown in Figure 4.2(b). The first function is the scaling function and the next two are the mother wavelet functions. Next four wavelet functions correspond to resolution level j=1. Similarly for higher resolution levels the first half of the wavelet functions are indexed according to the translations of the first mother wavelet and the second half corresponds to the translations of the second mother wavelet.

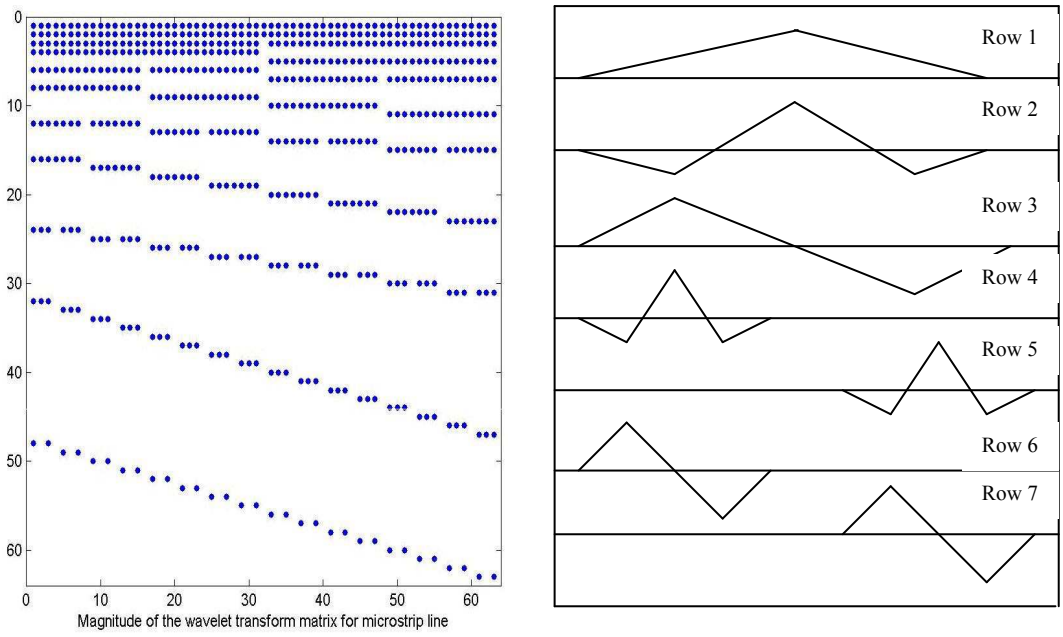

(a) (b)

Figure 4-2 a) Nonzero entries of the wavelet transform matrix for the chosen wavelet set with j=5. b) The shape of the first 7 functions of the wavelet system

When Figure 4.2(a) is investigated, it is observed that all the entries of W matrix are nonzero for the first three rows. This is due to the fact that these functions extend to the whole length of the microstrip line so each rooftop basis has a nonzero coefficient. On the other hand when the rows of W corresponding to higher resolution levels are considered, only the coefficients of rooftop functions that fall into the domain of the corresponding wavelet turn out to be nonzero.

To investigate the effects of threshold level, on the accuracy of solutions and the degree of sparsity, the analysis are performed at the same resolution level. The resolution level is chosen as 4, such that the number of wavelet functions for constructing the transformed MoM matrix is 31. The current distributions obtained for different threshold levels of 0.01, 0.005 and 0.001 are shown in Figure 4.3. As expected, with increasing threshold level, the resulting current distribution deviates from the actual one.

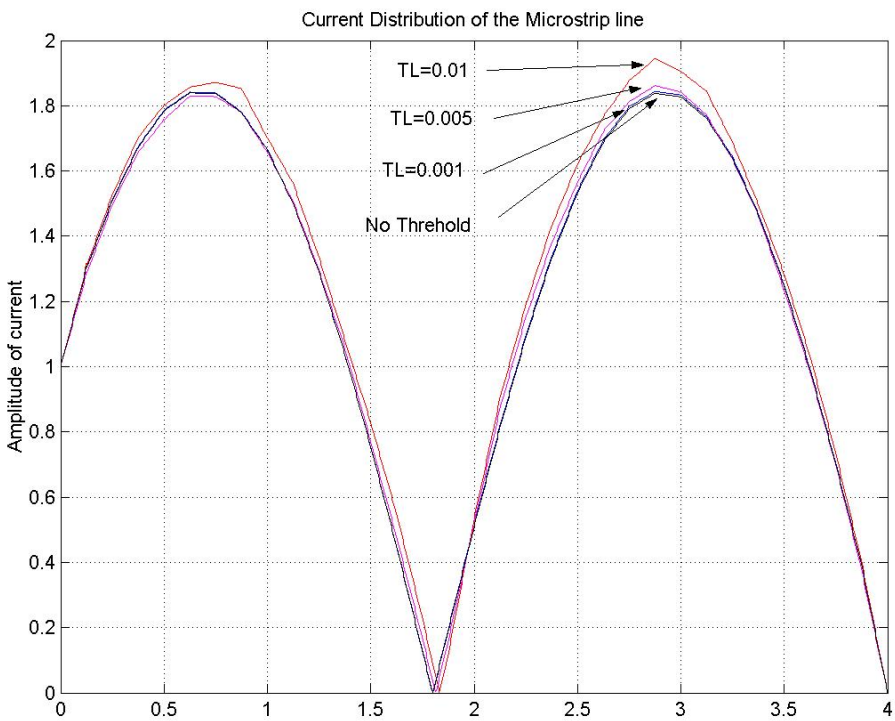

Figure 4-3 Effect of thresholding on the current distribution after applying different threshold levels (TL)

Figure 4.4 − 4.6 illustrate the sparsity patterns of the transformed MoM matrix for different threshold levels. The stars indicate the remaining nonzero elements. In Figures 4.4, 4.5, and 4.6, the degree of sparsity is 47%, 64% and 76%, for corresponding threshold levels 0.001, 0.005 and 0.01, respectively. It can be seen that in the choice of threshold level there is a trade-off between the degree of sparsity and the accuracy of the solutions. It is not easy to find some rules that are applicable to every problem. Therefore each different application should be investigated separately to find an appropriate threshold level according to the characteristics of the problem.

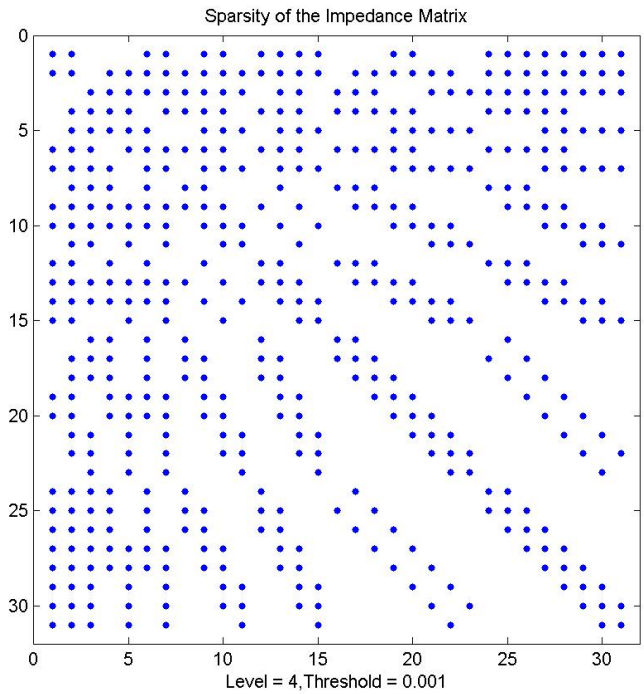

Figure 4-4 Sparsity pattern of the transformed impedance matrix,
Threshold = 0.001, Sparsity Ratio = 47%

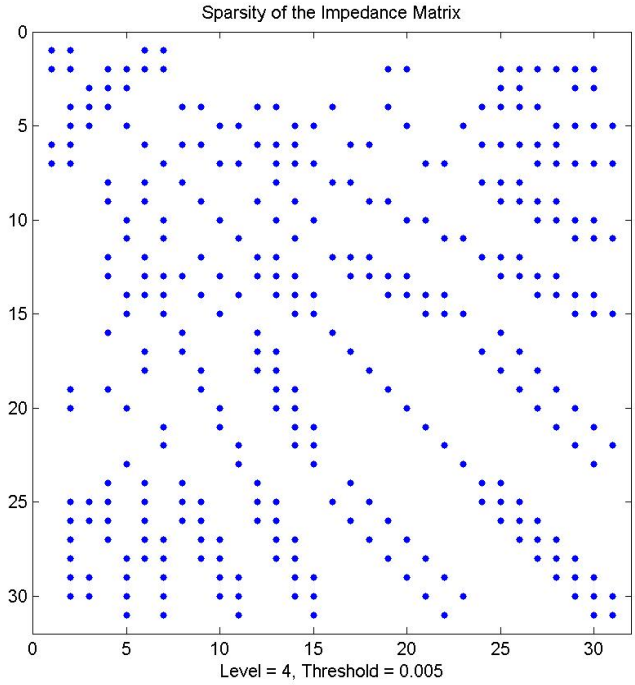

Figure 4-5 Sparsity pattern of the transformed impedance matrix, Threshold = 0.005, Sparsity Ratio = 64%

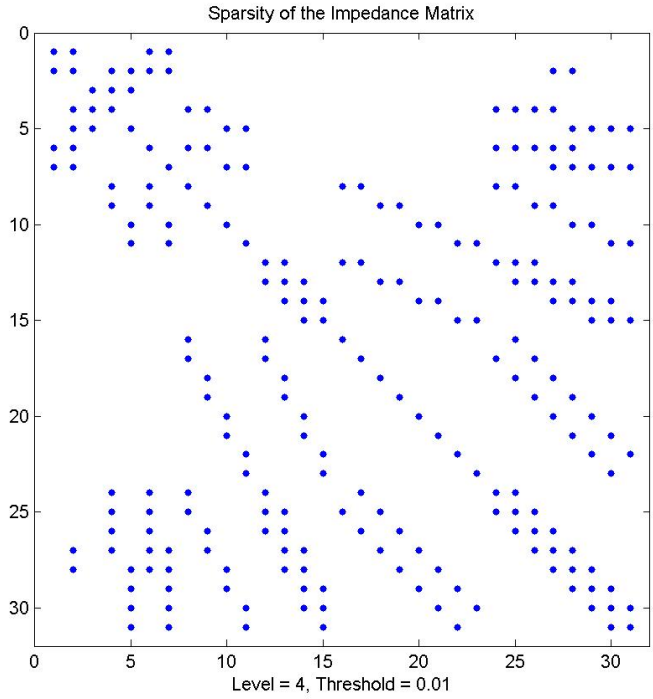

Figure 4-6 Sparsity pattern of the transformed impedance matrix, Threshold = 0.01, Sparsity Ratio = 76%

The reason why we obtain a sparse matrix by using wavelet basis functions is the zero average property of wavelet functions. An entry of a MoM matrix can be interpreted as the weighting of the electric field caused by the basis function. If the Green's function were constant, the electric field due to the zero-average wavelet function would be zero. But the Green's function varies rapidly for small distances between the source and observation points and it may be considered almost constant for larger distances. Therefore the matrix entries corresponding to large separation distance between the source and observation points become negligibly small, resulting in a sparse matrix after applying a threshold level.

In order to study the effects of other parameters on the degree of sparsity, the resolution level is increased to 5 so the number of basis functions becomes 63. The sparsity pattern of the impedance matrix is illustrated in Figures 4.7 and 4.8 for threshold levels 0.001 and 0.01 respectively.

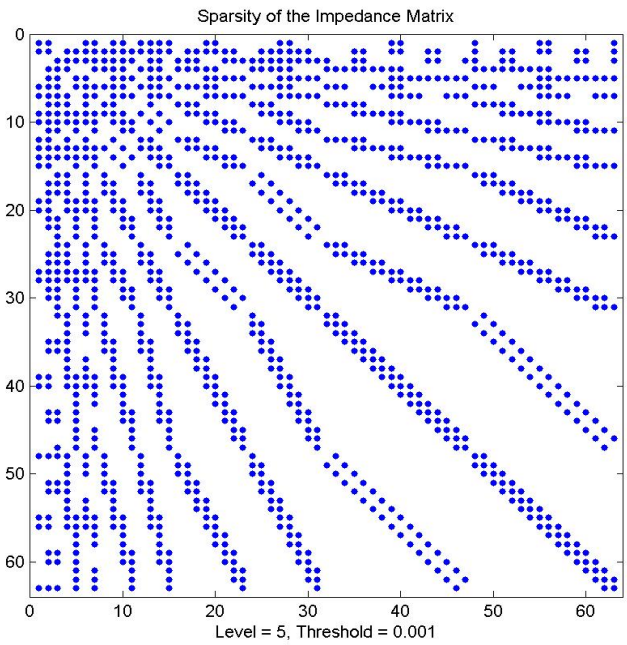

Figure 4-7 Sparsity pattern of the transformed impedance matrix, Threshold = 0.001, Sparsity Ratio = 68%

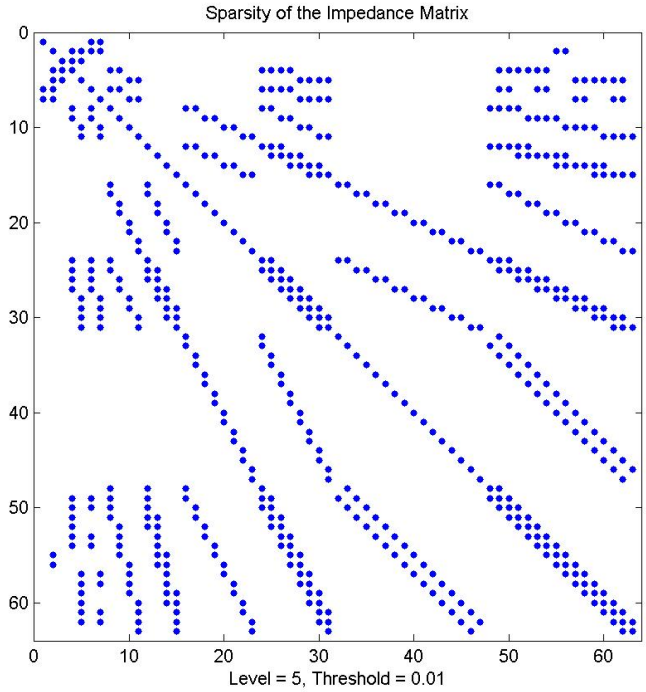

Figure 4-8 Sparsity pattern of the transformed impedance matrix,
Threshold = 0.01, Sparsity Ratio = 85%

Table 4-1 compares the degrees of sparsity obtained at different resolution levels for the same threshold values.

Table 4-1 Sparsity ratios

	Threshold Levels		
	TL=0.01	TL=0.005	TL=0.001
j= 4	76%	64%	47%
j= 5	85%	78%	68%

In order to better interpret why the degree of sparsity increases with increasing resolution level, Figure 4.2 that shows the structure of transformation matrix should be reconsidered. The number of zero entries increases with increasing resolution level. The increased number of zero entries at higher resolution level is

a consequence of this observation. Also intuitively one can easily conclude that as resolution level increases, the interaction between testing and basis functions at same resolution level but with different translation amounts will get smaller due to the increased distance between them.

The remaining part of the applied algorithm after the thresholding process is illustrated in Figure 4.9. As it is mentioned in Chapter 1, another advantage of converting the dense impedance matrix to a sparse matrix can be observed by implementing iterative matrix solvers that efficiently yield accurate solutions to some class of sparse matrix equations. There are different kinds of iterative solution methods like Gauss-Jacobi, Gauss-Seidel, Successive over relaxation, Conjugate gradient and its derivatives like Bi-Conjugate Gradient Method, Conjugate Gradient Squared Method and Bi-Conjugate Gradient Stabilized Method [25]. In this thesis Stabilized Bi-Conjugate Gradient Method (Bi-CGSTAB) which has already been implemented by MATLAB™ as a built in function will be utilized.

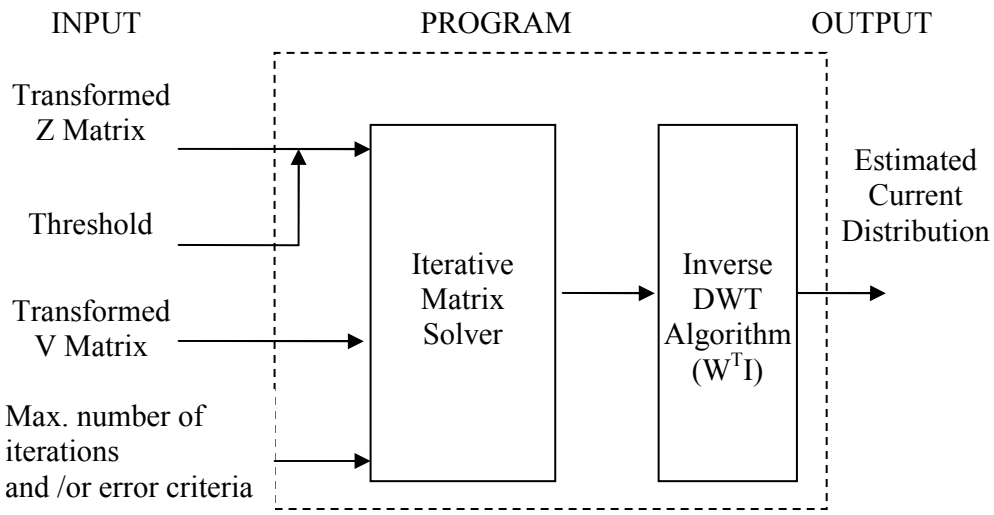

Figure 4-9 Solution procedure for the MoM matrix equation

The error criteria of Bi-CGSTAB algorithm is set to 0.001 and the number of iterations required to reach this error is compared for different resolution levels and threshold values. Table 4-2 summarizes the results obtained for the matrix equations constructed by using both rooftop and wavelet basis functions. Bi-CGSTAB algorithm requires two matrix vector products per iteration. The reason why we obtain halved values for the iteration number is due to the fact that the error criteria is satisfied at the end of the first matrix vector product for that iteration.

Table 4-2 Iteration Numbers

j=4	Threshold (0.01)	Threshold (0.005)	Threshold (0.001)
	Iteration	Iteration	Iteration
Matrix eqn. with rooftops	26.5	27.5	29.5
Matrix eqn. with wavelets	13.5	13.5	12.5
j=5	Threshold (0.01)	Threshold (0.005)	Threshold (0.001)
	Iteration	Iteration	Iteration
Matrix eqn. with rooftops	45.5	47.5	49.5
Matrix eqn. with wavelets	21.5	19.5	20.5

In Table 4.2, the iteration numbers obtained from the matrix equations with wavelets and rooftops for different resolution levels and different threshold values are given. In the same resolution level iteration numbers obtained from the matrix equation with rooftops are approximately two times greater than that obtained from the matrix equation with wavelets for the same threshold value. This faster convergence is obtained as a result of the sparsity pattern of the transformed impedance matrix. Furthermore when we increase the resolution level from 4 to 5, the iteration numbers obtained from both matrix equations increase. This is also the expected result because of enlarging the dimensions of the transformed at higher resolution levels.

After studying the microstrip line which is a one dimensional problem, as a more complicated two dimensional example microstrip patch antenna is considered. The rectangular patch antenna is fed with a center fed microstrip line positioned along the x-axis. The feed line is divided into 32 subdomains. On the other hand the microstrip patch is studied for different number of divisions in x and y directions. The three different cases studied for this example are summarized in Table 4-3.

Table 4-3 Number of divisions on the patch

	x-direction	y-direction
Case A	16	8
Case B	16	16
Case C	32	16

Recall that triangular wavelet system proposed in this thesis is used for the longitudinal variation of the current and Haar wavelet is used in the transverse direction. For triangular wavelet system, at the lowest resolution level there are three functions (1 scaling, 2 wavelets) corresponding four subdomains. On the other hand for the Haar wavelet system, there are two functions (1 scaling, 1 wavelet) corresponding to two subdomains. For each case the resolution levels for x directed and y directed currents are presented in Table 4-4.

Table 4-4 Resolution levels for x-directed and y-directed currents

	J_x		J_y	
	x-direction	y-direction	x-direction	y-direction
Case A	j=3	j=3	j=4	j=2
Case B	j=3	j=4	j=4	j=3
Case C	j=4	j=4	j=5	j=3

The indexing procedure was simpler for the microstrip line example but it is much more complicated for this two dimensional example. The indexing procedure is demonstrated in Table 4-5 and Table 4-6 for the x directed current with two resolution levels both in x and y directions.

Table 4-5 Individual indexing in x and y directions

x-direction defined wavelet	
Resolution Level	Index of wavelet function
j = 0	1
	2
	3
j =1	4
	5
	6
	7

y-direction Haar wavelet	
Resolution Level	Index of wavelet function
j =0	1
	2
j =1	3
	4

Table 4-6 Individual sub-indexing in x and y directions

x-direction		y-direction		Index of wavelet function for J_x
Level	Index	Level	index	
0	1	0	1	1
0	1	0	2	2
0	2	0	1	3
0	2	0	2	4
0	3	0	1	5
0	3	0	2	6
0	1	1	3	7
0	1	1	4	8

0	2	1	3	9
0	2	1	4	10
0	3	1	3	11
0	3	1	4	12
1	4	0	1	13
1	4	0	2	14
1	5	0	1	15
1	5	0	2	16
1	6	0	1	17
1	6	0	2	18
1	7	0	1	19
1	7	0	2	20
1	4	1	3	21
1	4	1	4	22
1	5	1	3	23
1	5	1	4	24
1	6	1	3	25
1	6	1	4	26
1	7	1	3	27
1	7	1	4	28

For the y directed current a similar procedure is applied, only the x direction and y direction labels are interchanged in Table 4-5 for J_y.

In Figures 4.9−4.11 sparsity patterns of the transformed matrices are presented for three different cases and two threshold constants. During the thresholding process each partition of MoM matrix (Z_{xx}, Z_{xy}, Z_{yx}, Z_{yy}) are evaluated according to the maximum value of that partition. The first 32 rows and columns of the MoM matrix correspond to the basis and testing functions on the microstrip feed line. The other part corresponds to the basis functions on the patch. Therefore it is more

appropriate to consider those remaining parts when comparing different resolution levels on the patch.

In Figure 4-11 it can be observed that the sparsity patterns for Z_{xx} and Z_{yy} (and also for Z_{xy} and Z_{yx}) are same. This is an expected result since in this case, the resolution levels in longitudinal and transverse directions are same for x and y directed currents. It is seen in Figure 4.10 that the Z_{xx} part of the matrix is same as the first ¼ of the matrix in Figure 4.11. The similar behavior is also observed for other partitions of the matrix and also for the higher resolution case given in Figure 4.12. This is also an expected result of multiresolution analysis. As we increase the resolution level, nothing is changed for the lower resolution levels. This is one of the most important advantages of MRA. In traditional analysis, when we increase the resolution by increasing the number of divisions, all the entries of the MoM matrix change. Therefore one needs to calculate the whole matrix for different resolution levels. But in MRA, when the resolution level is increased by one, ¼ of the matrix remains same, only the additional entries need to be evaluated. This property of MRA is also used to test the software developed for the simulations. The transformed matrices for Case A and Case B are obtained from two different MoM matrices that are obtained by using rooftop basis with different sizes.

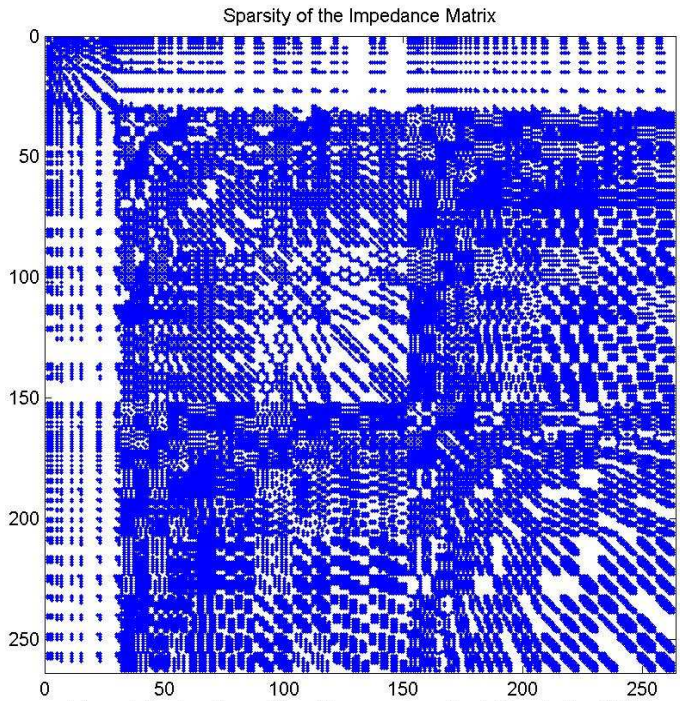

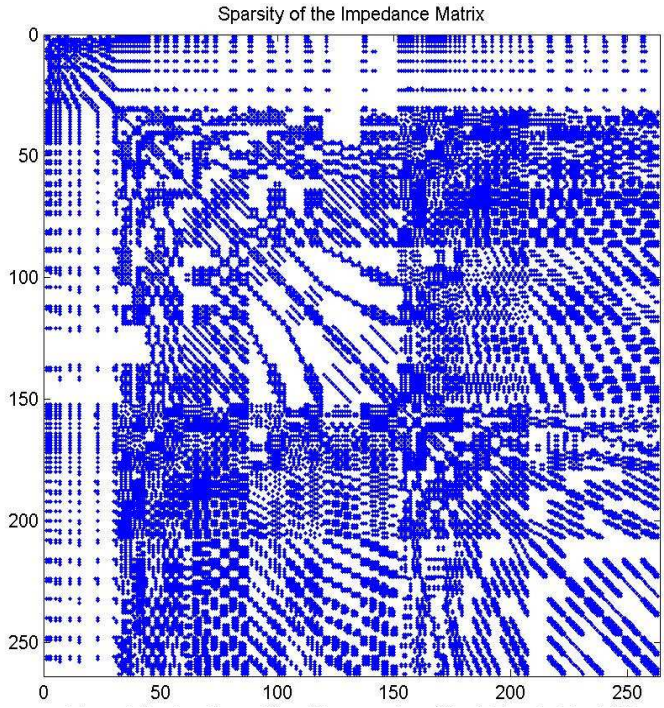

Figure 4-10 Sparsity of the impedance Matrix, Case 1,
Different threshold values (a) 0.0001, (b) 0.001
Sparsity Ratios (a) 48%, (b) 64%

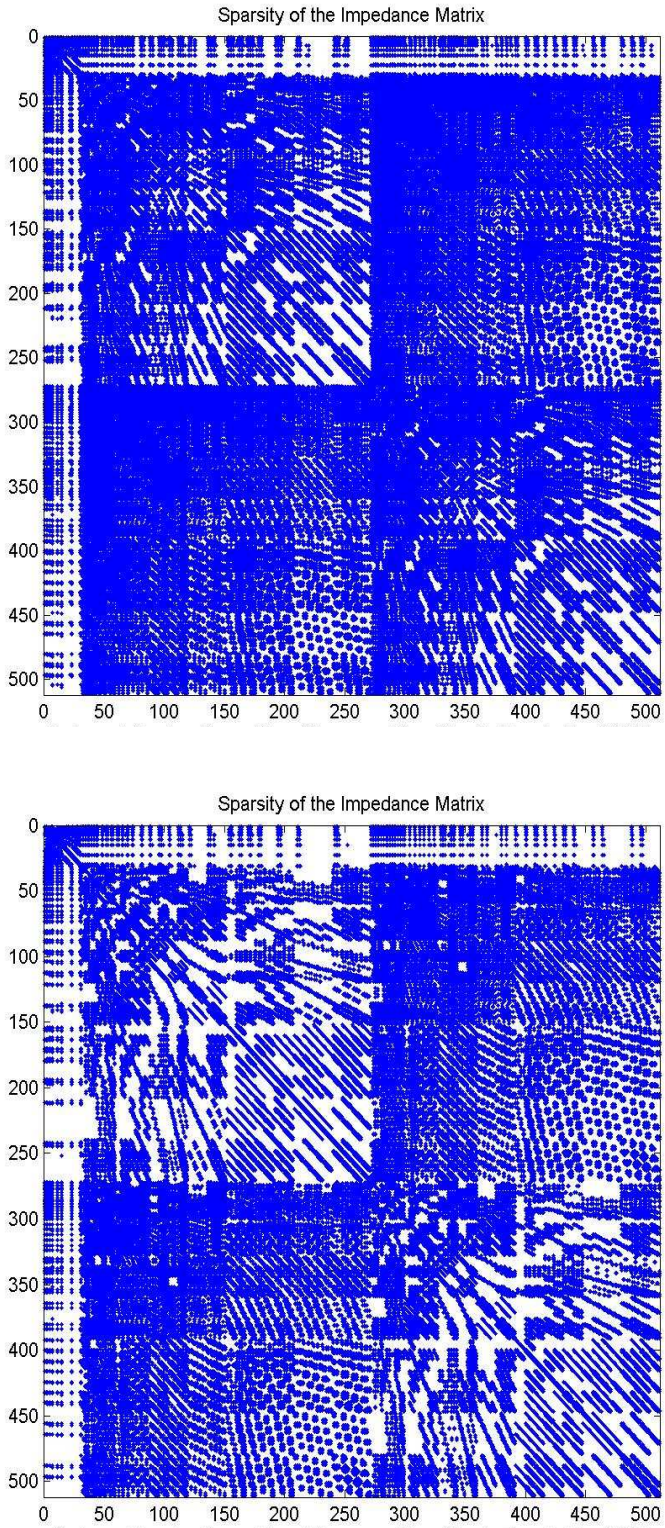

Figure 4-11 Sparsity of the impedance Matrix, Case 2,
Different threshold values (a) 0.0001, (b) 0.001
Sparsity Ratios (a) 58%, (b) 73%

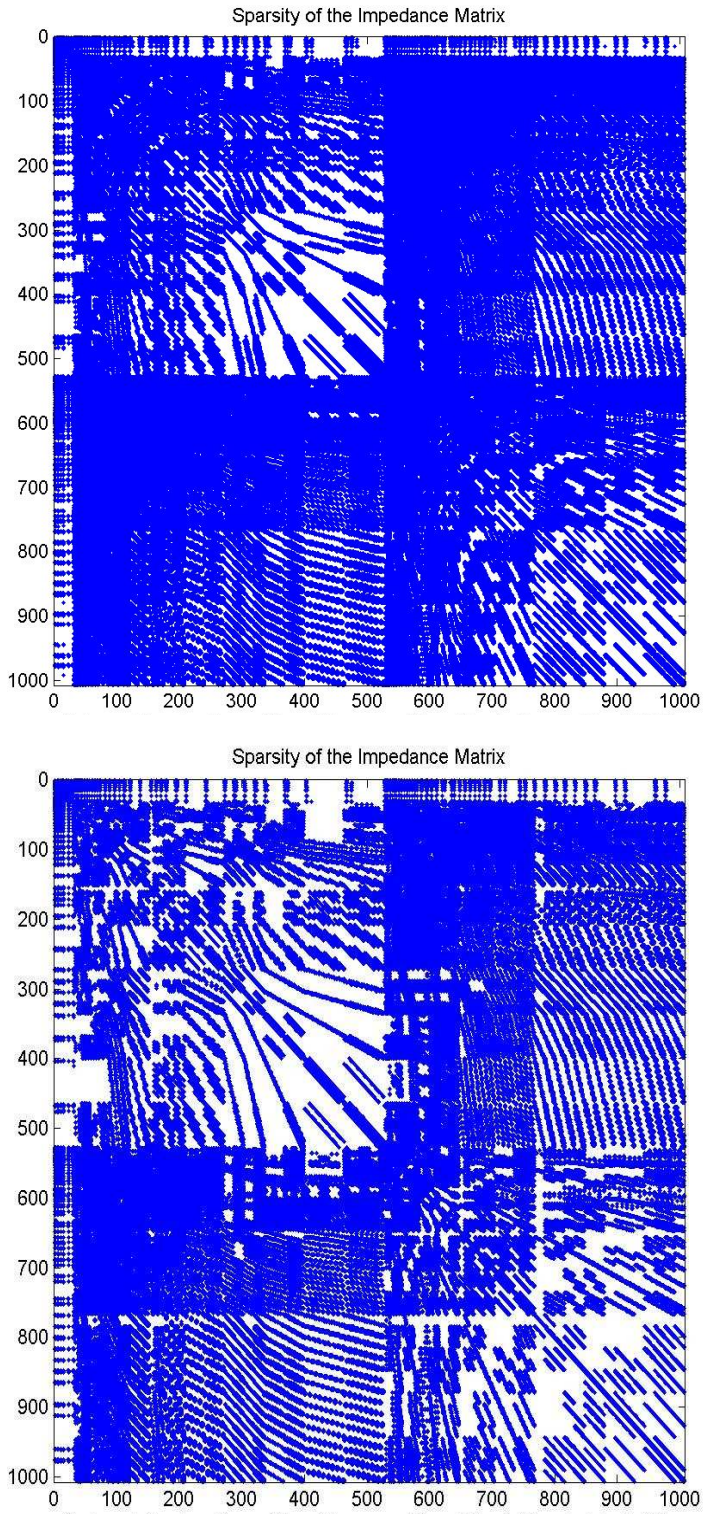

Figure 4-12 Sparsity of the impedance Matrix, Case 3,
Different threshold values (a) 0.0001, (b) 0.001
Sparsity Ratios (a) 70%, (b) 83%

After the transformation, when the corresponding matrix entries of two matrices of Case A and Case B are compared, it is observed that they are almost same as expected.

Another test data used to verify the developed software is the current solution vector. As it is discussed in Chapter 2, in MRA details are captured at higher resolution levels. Therefore when the entries of a solution vector at two different resolution levels are compared, the entries corresponding to the same level should be same. In order to make such a comparison the first 50 entries of the current solution vector (the parts corresponding to the currents on the patch) for the transformed matrix equation are plotted in Figures 4.13 and 4.14 for different resolution levels. It can be observed that the results are almost same as expected.

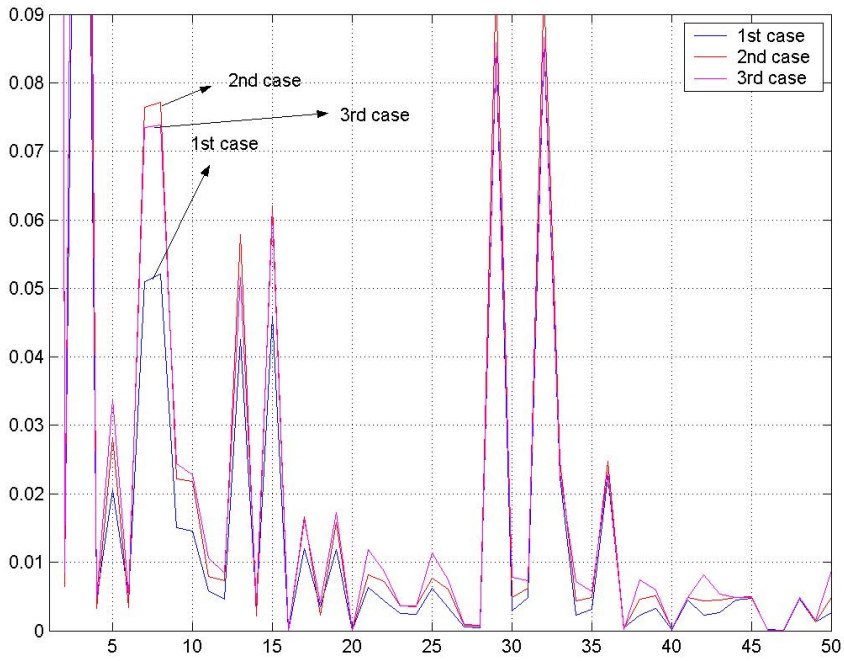

Figure 4-13 The current solution vector for different resolutions along the x-axis

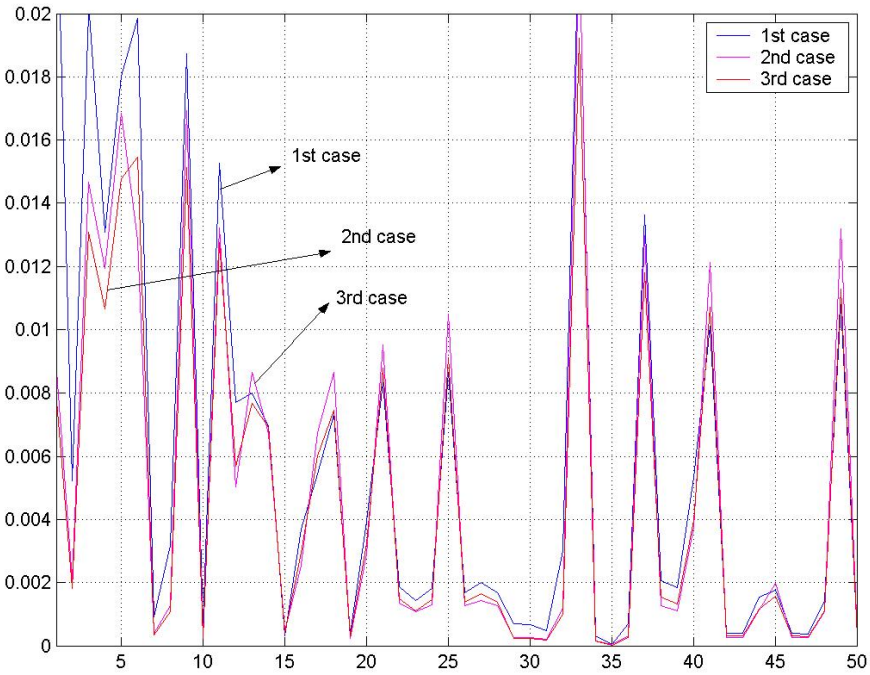

Figure 4-14 The current solution vector for different resolutions along the y-axis

Finally, the transformed matrix equations are solved by using Bi-CGSTAB method with an error criterion 0.001. The number of iterations for different resolution levels and threshold values are presented in Table 4-7. The results are not as expected. First of all when the results of the one dimensional problem and this two dimensional example are compared, it may be concluded that wavelet basis does not perform well for the two dimensional case. The main reason for this observation may be the partitioned nature of the MoM matrix and a low degree of sparsity obtained for the Z_{xy} and Z_{yx} partitions.

The main reason for the low performance of the proposed wavelet system may be its non-orthogonal nature. When the piecewise linear wavelet systems studied in literature are investigated it is seen that they are either Battle-Lemarie or B-spline wavelet systems [22]. In Battle-Lemarie system the wavelet functions have infinite support and they form an orthogonal set. On the other hand, B-spline wavelets

have compact supports but they result in a semi-orthogonal system. Because of the ease in evaluating the matrix entries, compactly supported wavelets are preferred in this thesis. When B-spline wavelets are considered, different wavelet functions need to be defined for the boundaries. In this thesis a wavelet system with same functions all over the solution space is aimed. The proposed system meets this requirements but it results in a non-orthogonal system. It can be concluded that the iteration numbers presented in Table 4-7 demonstrate the importance of designing an orthogonal wavelet system for better performance of multiresolution analysis.

The condition numbers that are given in Table 4-7, are the 2-norm condition numbers. 2-norm condition number means the ratio of the largest singular value of transformed sparse matrix to the smallest. Large condition numbers indicate an ill condition.

Table 4-7 Iteration numbers and Condition Numbers for different resolution and threshold values

Case 1	Threshold (0.001)		Threshold (0.0001)	
	Iteration	Cond. Number	Iteration	Cond. Number
Matrix eqn. with rooftops	158.5	100	109.5	166.66
Matrix eqn. with wavelets	419.5	28908	357.5	23215
Case 1	No Threshold			
	Iteration	Cond. Number		
Matrix eqn. with rooftops	120.5	95		
Matrix eqn. with wavelets	566.5	131752		
Case 2	Threshold (0.001)		Threshold (0.0001)	
	Iteration	Cond. Number	Iteration	Cond. Number
Matrix eqn. with rooftops	123	44	107.5	44
Matrix eqn. with wavelets	3807.5	20487	820	30019
Case2	No Threshold			
	Iteration	Cond. Number		
Matrix eqn. with rooftops	104.5	44		
Matrix eqn. with wavelets	1248	1.0297e+5		
Case 3	Threshold (0.001)		Threshold (0.0001)	
	Iteration	Cond. Number	Iteration	Cond. Number
Matrix eqn. with rooftops	308.5	106	184.5	97
Matrix eqn. with wavelets.	>10000	69602	2818.5	61092
Case 3	No Threshold			
	Iteration	Cond. Number		
Matrix eqn. with rooftops	217.5	98		
Matrix eqn. with wavelets.	2998.5	3.0194e+7		

CHAPTER 5

CONCLUSION

A major aim of methodology presented in this thesis is the effective use of the wavelet basis functions in the MoM analysis of printed structures. In this thesis, first recent studies on wavelets in computational electromagnetics are searched. The applications of wavelets in electromagnetic problems and studies with different wavelet functions are examined. Then the multiresolution analysis is presented and an example of using Haar wavelets in multiresolution analysis is illustrated. The conditions for constructing the multiresolution analysis are investigated by the Haar wavelets. The mixed potential integral equation used in the analysis of microstrip structures is defined and the classical MoM solution of integral equations is reviewed. A new wavelet system for the expansion of the surface currents in the longitudinal direction is proposed and the Haar wavelet set is used in transverse direction. The wavelet set proposed for the longitudinal direction completely spans the same space as the classical rooftop basis set. It is well known that use of traditional basis functions like rooftop functions results in a dense MoM matrix. When the analysis of electrically large structures like a microstrip patch antenna array is considered, the solution of the dense MoM matrix equation requires excessive memory and CPU time usage. On the other hand, wavelet basis functions result in a sparse matrix equation due to their special features like having zero average. Wavelet basis functions can be utilized in two different ways; either by directly evaluating the matrix entries for the wavelet basis or by transforming the MoM matrix obtained for the rooftop basis via the use of DWT. Both methods result in the same matrix but the latter method is found to be computationally more efficient.

The method is first applied to the analysis of microstrip lines, which is a one-dimensional problem. Depending on the resolution and threshold levels a

considerable amount of sparsity could be achieved. The sparse matrix equation is solved by using the iterative Bi-CGSTAB method. When the number of iterations required for the solution of the MoM matrix with rooftop basis functions is compared to the one with wavelet basis functions, it is observed that the transformed matrix performs better.

Then, the method is applied to analyze a two-dimensional problem that is a microstrip patch antenna. For this case a similar sparsity level is obtained as for the one-dimensional problem. However the matrix solution did not converge up to a large number of iterations. In order to investigate the causes of this unexpected behavior, first the developed software is verified by using some properties of multiresolution analysis. After this verification it is concluded that the proposed wavelet system may not be a good choice since it does not form an orthogonal system. As a future work other compactly supported and piecewise linear wavelet systems will be studied to end up with a wavelet basis set that could further improve the efficiency of MoM analysis for printed structures.

REFERENCES

[1] R. F. Harrington, *Field Computations by Moment Methods*, New York: Macmillan, 1968.

[2] J. Jin, *The Finite Element Method in Electromagnetics*, New York: John Willey & Sons, Inc, 1993.

[3] A. Taflove, *Computational Electrodynamics: The Finite Difference Time Domain Method*, Boston: Artech House, Inc, 1995.

[4] R. E. Miller, "Electromagnetic Integral Equations with Wavelets", Ph. D. Dissertation, Texas A&M University, August 1999.

[5] K. F. Sabet and L. P. B. Katehi, "An Integral Formulation of Two- and Three Dimensional Dielectric Structures Using Ortonormal Multiresolution Expansion", *International Journal of Numerical Modeling: Electronic Networks, Devices and Fields*, Vol. 11, pp.3-19, 1998.

[6] B. Z. Steinberg and Y. Leviatan, "On the Use of Wavelet Expansions in the Method of Moments", *IEEE Transactions on Antennas and Propagation*, Vol.41, No.5, pp. 610-619, 1993.

[7] Z. Baharav and Y. Leviatan, "Wavelets in Electromagnetics: The impedance Matrix Compression (IMC) Method", *International Journal of Numerical Modeling: Electronic Networks, Devices and Fields*, Vol. 11, pp. 69-84, 1998.

[8] "R. L. Wagner, W. C. Chew, "A Study of Wavelets for the Solution of Electromagnetic Integral Equations", *IEEE Trans. on Antennas and Propagation*, Vol. 43, No. 8, pp. 802-810, 1995.

[9] R. L. Wagner, G. P. Otto and W. C. CHEW, "Fast Waveguide Mode Computation Using Wavelet-Like Basis Functions", *IEEE Microwave and Guided Wave Letters*, Vol. 3, No. 7, pp.208-210, 1993.

[10] J. C. Goswami, A. K. Chan and C. K. Chui, "On Solving First-Kind Integral Equations Using Wavelets on a Bounded Interval", *IEEE Transactions on Antennas and Propagation*, Vol. 43, No.6, pp.614-622, 1995.

[11] W. Y. Tam, "Weighted Haar wavelet-like basis for scattering problems", *IEEE Microwave and Guided Wave letters*, pp. 435-437, 1996.

[12] K. F. Sabet, J. -C. Cheng and L. P. B. Katehi, "Efficient wavelet-based modeling of printed circuit antenna arrays", *IEE Proc. -Microwave Antennas Propag.* , Vol. 146, No.4, pp.298-304, 1999.

[13] Z. Xiang and Y. Lu, "An Effective Wavelet Matrix Transform Approach for Efficient Solutions of Electromagnetic Integral Equations", *IEEE Transactions on Antennas and Propagation*, Vol.45, No. 8, pp.1205-1203, 1997.

[14] W. C. CHEW, J.-M. JIN, C.-C. LU, E. Michielssen and J. M. SONG, "Fast Solution Methods in Electromagnetics", *IEEE Transactions on Antennas and Propagation*, Vol.45, No. 3, pp.533-543, 1997.

[15] K. Kalbasi and K. R. Demarest, "A Multilevel Formulation of the Method of Moments", *IEEE Transactions on Antennas and Propagation*, Vol.41, No.5, pp.589-599, 1993.

[16] R.Polikar,http://users.rowan.edu/~polikar/WAVELETS/WTtutorial.html; August 2004.

[17] C. S. Burrus, R. A. Gopinath and H. Guo, *Introduction to wavelets and wavelet transforms*, Prentice Hall, 1998.

[18] L. M. T. Carvalho., L. M. G. Fonseca, F. Murtagh and J. G. P. W. Clevers, "Changes at Multiple Spatial Scales*", Industrial and Academic Research Proposition Showcase*, Vol. 33, Amsterdam, 2000.

[19] Robert D. Nevels, J. C. Goswami and H. Tehrani, "Semi-orthogonal versus Orthogonal Wavelet Basis Sets for Solving Integral Equations", *IEEE Transactions on Antennas and Propagation*, Vol. 45, No.9, pp.1332-1339, 1997.

[20] J. F. Zurcher, F. E. Gardiol, *Broadband patch antennas*, Artech House, Boston 1995.

[21] P. Bhartia, I. Bahl, R. Garg, A. Ittipiboon, *Microstrip Antenna Design Handbook*, Artech House Antennas and Propagation Library, 2001.

[22] Y. L. Chow, J.J. Yang, and D. F. Fang and G. E. Howard, "Closed form spatial Green's function for the thick substrate", *IEEE Trans. Microwave Theory Tech*., Vol. MTT-39, No. 3, pp. 588-592, 1991.

[23] M. I. Aksun, "A robust approach for the derivation of the closed form Green's functions", *IEEE Trans. Microwave Theory Tech*., Vol. MTT-45, No. 5, 1996.

[24] M. I. Aksun and R. Mittra, "Choices of expansion and testing functions for the method of moments applied to a class of electromagnetic

problems", *IEEE Trans. Microwave Theory Tech.*, vol. MTT-41, pp. 503-509, 1993.

[25] N. ÜNSOY, "Development of a software involving a group of iterative solvers and preconditioners for sparse matrix equations of computational electromagnetics", MS Thesis, Middle East Technical University, September 2001.